Generic Argillite/Shale Disposal Reference Case

Fuel Cycle Research & Development

Prepared for

U.S. Department of Energy
Used Fuel Disposition Campaign

Liange Zheng[1]
Carlos Jové Colón[2]
Marco Bianchi[1]
Jens Birkholzer[1]

[1] Lawrence Berkeley National Laboratory
[2] Sandia National Laboratory

August, 2014

FCRD-UFDC-2014--000319

Revision 2
12/20/2012

APPENDIX E

FCT DOCUMENT COVER SHEET [1]

Name/Title of Deliverable/Milestone/Revision No.	Generic Argillite/Shale Disposal Reference Case
Work Package Title and Number	DR Generic Disposal System Analysis – LBNL FT-14LB080802
Work Package WBS Number	1.02.08.08
Responsible Work Package Manager	Jens Birkholzer

(Name/Signature)

Date Submitted 08/08/2014

Quality Rigor Level for Deliverable/Milestone[2]	☐ QRL-3	☐ QRL-2	☐ QRL-1 ☐ Nuclear Data	☒ Lab/Participant QA Program (no additional FCT QA requirements)

This deliverable was prepared in accordance with Lawrence Berkeley National Laboratory
(Participant/National Laboratory Name)

QA program which meets the requirements of
☒ DOE Order 414.1 ☐ NQA-1-2000 ☐ Other

This Deliverable was subjected to:

☐ Technical Review ☐ Peer Review

Technical Review (TR) **Peer Review (PR)**

Review Documentation Provided **Review Documentation Provided**

☐ Signed TR Report or, ☐ Signed PR Report or,
☐ Signed TR Concurrence Sheet or, ☐ Signed PR Concurrence Sheet or,
☐ Signature of TR Reviewer(s) below ☐ Signature of PR Reviewer(s) below

Name and Signature of Reviewers

NOTE 1: *Appendix E should be filled out and submitted with the deliverable. Or, if the PICS:NE system permits, completely enter all applicable information in the PICS:NE Deliverable Form. The requirement is to ensure that all applicable information is entered either in the PICS:NE system or by using the FCT Document Cover Sheet.*

NOTE 2: *In some cases there may be a milestone where an item is being fabricated, maintenance is being performed on a facility, or a document is being issued through a formal document control process where it specifically calls out a formal review of the document. In these cases, documentation (e.g., inspection report, maintenance request, work planning package documentation or the documented review of the issued document through the document control process) of the completion of the activity along with the Document Cover Sheet is sufficient to demonstrate achieving the milestone. If QRL 1, 2, or 3 is not assigned, then the Lab/Participant QA Program (no additional FCT QA requirements box must be checked, and the work is understood to be performed, and any deliverable developed, in conformance with the respective National Laboratory/Participant, DOE- or NNSA-approved QA Program..*

This page is intentionally blank.

CONTENTS

FIGURES

TABLES

ACRONYMS

BWR	Boiling Water Reactor
DPC	Dual Purpose Canister
DSEF	Disposal Systems Evaluation Framework
EDZ	Excavation Disturbed Zone
EBS	Engineered Barrier System
FE	Full-Scale Emplacement Experiment
FEBEX	Full-scale Engineered Barriers EXperiment
HC	Hydrological and Chemical
HM	Hydrological and Mechanical
HLW	High-Level Waste
IRF	Instant Release Fraction
MC	Mechanical and Chemical
MTHM	Metric Tons Heavy Metal
NBS	Natural Barrier System
OoR	Out-of-Reactor
PA	Performance Assessment
PWR	Pressurized Water Reactor
SNF	Spent Nuclear Fuel
TH	Thermal and Hydrological
TC	Thermal and Chemical
TM	Thermal and Mechanical
THM	Thermal, Hydrological and Mechanical
THMC	Thermal, Hydrological, Mechanical and Chemical
UFDC	Used Fuel Disposition Campaign
UNF	Used Nuclear Fuel
URLs	Underground Research Laboratories
WIPP	Waste Isolation Pilot Plant

1. Introduction

Radioactive waste disposal in a deep subsurface repository hosted in clay/shale/argillite is a subject of widespread interest given the desirable isolation properties, geochemically reduced conditions, and widespread geologic occurrence of this rock type (Hansen 2010; Bianchi et al. 2013). Bianchi et al. (2013) provides a description of diffusion in a clay-hosted repository based on single-phase flow and full saturation using parametric data from documented studies in Europe (e.g., ANDRA 2005). The predominance of diffusive transport and sorption phenomena in this clay media are key attributes to impede radionuclide mobility making clay rock formations target sites for disposal of high-level radioactive waste. The reports by Hansen et al. (2010) and those from numerous studies in clay-hosted underground research laboratories (URLs) in Belgium, France and Switzerland outline the extensive scientific knowledge obtained to assess long-term clay/shale/argillite repository isolation performance of nuclear waste. In the past several years under the UFDC, various kinds of models have been developed for argillite repository to demonstrate the model capability, understand the spatial and temporal alteration of the repository, and evaluate different scenarios. These models include the coupled Thermal-Hydrological-Mechanical (THM) and Thermal-Hydrological-Mechanical-Chemical (THMC) models (e.g. Liu et al. 2013; Rutqvist et al. 2014a, Zheng et al. 2014a) that focus on THMC processes in the Engineered Barrier System (EBS) bentonite and argillite host hock, the large scale hydrogeologic model (Bianchi et al. 2014) that investigates the hydraulic connection between an emplacement drift and surrounding hydrogeological units, and Disposal Systems Evaluation Framework (DSEF) models (Greenberg et al. 2013) that evaluate thermal evolution in the host rock approximated as a thermal conduction process to facilitate the analysis of design options. However, the assumptions and the properties (parameters) used in these models are different, which not only make inter-model comparisons difficult, but also compromise the applicability of the lessons learned from one model to another model. The establishment of a reference case would therefore be helpful to set up a baseline for model development. A generic salt repository reference case was developed in Freeze et al. (2013) and the generic argillite repository reference case is presented in this report. The definition of a reference case requires the characterization of the waste inventory, waste form, waste package, repository layout, EBS backfill, host rock, and biosphere. This report mainly documents the processes in EBS bentonite and host rock that are potentially important for performance assessment and properties that are needed to describe these processes, with brief description other components such as waste inventory, waste form, waste package, repository layout, aquifer, and biosphere. A thorough description of the generic argillite repository reference case will be given in Jové Colón et al. (2014).

2. Generic Argillite Repository Disposal Concept

The reference case for clay/shale/argillite is largely consistent with that developed for the generic salt repository disposal concept (Freeze et al. 2013), with some modifications to meet the requirement for an argillite repository. Specific assumptions of the generic argillite disposal concept are the following:

- Waste disposal capacity is 70,000 metric tons of heavy metal (MTHM).
- Horizontal repository layout consists of excavated emplacement drifts or tunnels separated by the clay host rock with a centralized access hallway (Figure 1):
  - Waste package spacing and drift spacing are dictated by total radionuclide inventory, waste package size, engineered barrier system configuration, and thermal loading.
- Horizontal disposal galleries (see Figure 2) are emplaced end-to-end with waste packages in drifts that are lined with cement (see Figure 3) and/or metal support structures. Disposal galleries are then backfilled with clay material. Multilayered backfilling is part of the engineered barrier system (see Figure 3).

- Ground support structures and cement linings (see Figure 3) are needed. The properties of the lining (rigidity, pervious/impervious) depends on the mechanical and hydrologic properties of the clay rock.
- Drifts and centralized access hallways are sealed at closure. Drift and central access design layout can vary depending on waste type, heat loads, and canister size.
- Access shafts are used for construction, waste handling operations, and ventilation. They will be sealed at closure.
- Excavated drifts will be emplaced at a depth of about 650 meters within a clay rock unit. Given the anticipated heterogeneities in shale formations, the presence of either bentonite clay strata or other lithologic units should be accounted for.

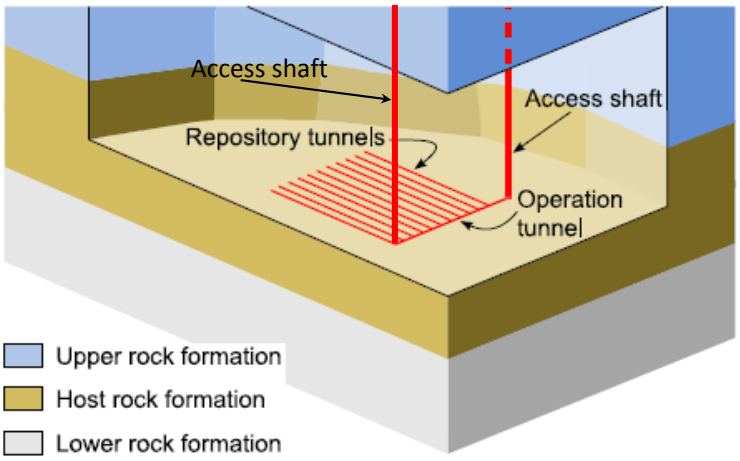

Figure 1. Generic design for a deep geological nuclear waste repository in shale (Modified after Bianchi et al. (2013)).

Repository design will meet operational requirements to guarantee safe pre- and post-closure performance. Pre-closure operational constraints encompass shaft dimensions for access and ventilation during mining activities, transport, emplacement of waste packages, sealing, and monitoring. Hardin (2014; Review of Underground Construction Methods and Opening Stability for Repositories in Clay/Shale Media) provides a review of excavation and construction practices of underground tunnels in clay/shale rock media. This study is part of a feasibility evaluation for the direct disposal of SNF in large heat-generating DPCs. The report summarizes the experience (about 50 years or more) and technological viability garnered in the construction of large-diameter and long tunnels for vehicle transportation (highways, railroads) and underground water passages in the USA and Europe. Einstein (2000) provides a good summary of tunneling activities and potential issues (clay softening and swelling) in the construction of tunnels in Opalinus clay/shale. Einstein (2000) also provides important points of consideration on recent tunnel construction methods such as the use of circular tunnel cross-sections (reduced shear stress) and the emplacement of pre-fabricated liners that are evenly-arranged and water-tight to preclude water ponding and its movement from the rock.

Drift spacing will be constrained by the dimensions of pillar structures to support safe underground tunneling (preclude drift collapse) and pre-closure operations during emplacement. Drift spacing and in-drift spacing between waste packages will be constrained by thermal loading on compliance points relative to coordinate locations of waste packages in the drift and the clay host rock. At this point, compliance points are defined as ‘observation’ points for temperature-time profiles located within the

drift (e.g., drift wall, buffer, and waste package surface) or within the host rock at a defined distance from the drift wall represented by temperatures at a given time. The current treatment of compliance points is arbitrary and it is used mainly for evaluation of thermal loads for a given type of waste and package size (Greenberg et al. 2013). The use of compliance points would be key to the evaluation of thermal limits combined with other knowledge on EBS material properties and thermal characteristics, and host-rock thermal-hydrologic (TH) properties

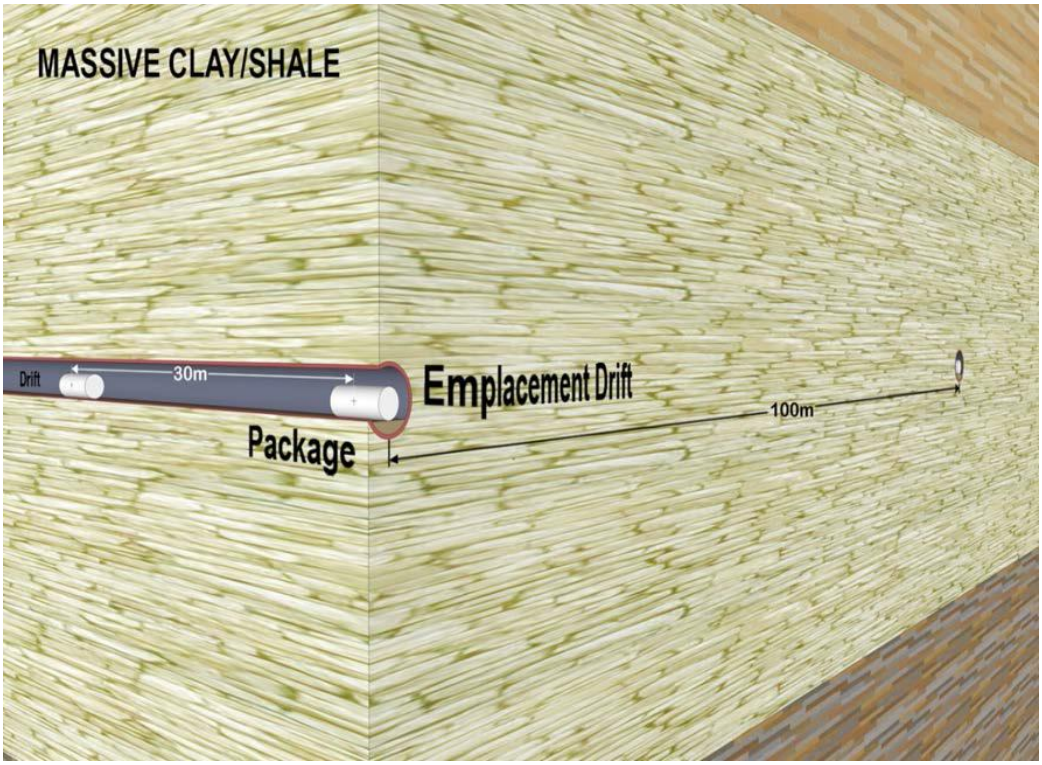

Figure 2. Schematic illustration of an emplacement drifts for an argillite-hosted repository (Hardin et al. 2013). Note that Hardin et al. (2013) determined drift and waste package spacing based on a thermal limit at the rock wall of 100°C. In this report smaller spacing is used based on the scoping calculation by Greenberg et al. (2013).

3. Generic Argillite Repository Reference Case

The generic crystalline repository reference case has the following major elements:

- Waste inventory
- Engineered barrier system
  - Waste form
  - Waste package
  - Repository layout
  - Backfill
  - Seals
- Natural barrier system
- Biosphere

In this report, we briefly describe the waste inventory, waste form, waste package, repository layout, and biosphere, with more thorough description of these elements given in Jové Colón et al. (2014). Backfill and natural barrier system are the focus of this report.

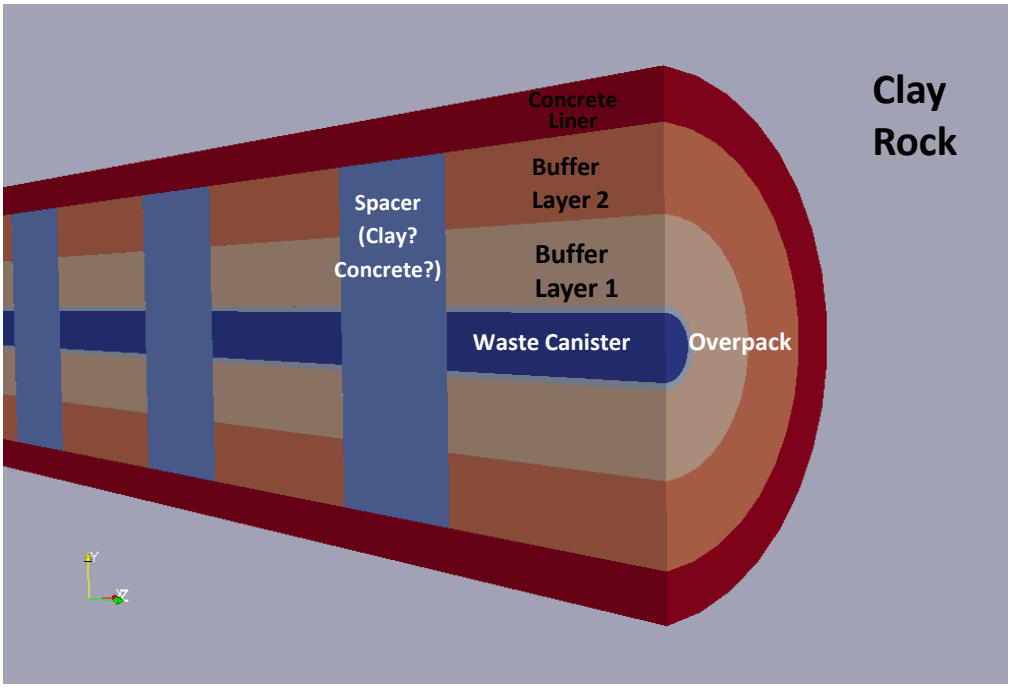

Figure 3. Schematic representation of a circular cross-section of a single drift with multiple waste canisters and a multi-layered EBS.

3.1 Waste Inventory

Waste inventory assumed in the reference case has been discussed in Freeze et al. (2013) for the salt disposal system. The same inventory is also assumed for the argillite reference case. We therefore briefly discussed the waste inventory in this section and reference details to Freeze et al. (2013).

Just like salt reference case, repository capacity for the argillite reference case for is 70,000 metric tons heavy metal (MTHM). For simplicity, the entire single-repository inventory is assumed to consist of pressurized water reactor (PWR) used nuclear fuel (UNF) assemblies. Each PWR UNF assembly contains 0.435 MTHM (91,000 MTHM/209,000 assemblies). The single-repository reference case PWR inventory assumes a bounding fuel burn-up 60 GWd/MTHM. The isotopic composition of the reference case 60 GWd/MTHM PWR inventory assumes an initial enrichment of 4.73% and 30-year out-of-reactor (OoR) decay storage, as reported in Carter et al. (2012, Table C-1). This reference case inventory can be augmented with boiling water reactor (BWR) and high-level waste (HLW) inventories as the performance assessment (PA) model matures.

The reference case PWR UNF inventory includes approximately 450 isotopes with a total mass of 1.44×10^{6} g/MTHM and a decay heat of 1.438 kW/MT (Carter et al. 2012, Table C-1). The total mass of the PWR inventory includes actinides (dominated by ^{238}U), oxygen from the UO_2, zirconium from cladding, and other fission and activation products. The mass inventory of these selected radionuclides in a reference case PWR UNF assembly (60 GWd/MTHM burn-up, 30-year OoR, 4.73% initial enrichment) is shown in Table 1.

Smaller subset of radionuclides that are considered in the salt reference case (Freeze et al. 2013) are also assumed for the argillite reference case, including neptunium series alpha-decay chain, uranium series

alpha-decay chain, and ^{129}I, a non-sorbing radionuclide with a long half-life. Details of their half-life and decay constants are given in Freeze et al. (2013).

Table 1. UNF Radionuclide Inventory for the Reference Case (same as Table 3-1 in Freeze et al., 2013)

Isotope	Waste inventory mass[1] (g/MTHM)	Molecular weight[2] (g/mol)	Mass fraction[2] (g / g UNF)	Mole fraction (mol / g UNF)
^{238}U	9.10×10^{5}	238.05	6.32×10^{-1}	2.66×10^{-3}
^{237}Np	1.24×10^{3}	237.05	8.61×10^{-4}	3.63×10^{-6}
^{241}Am	1.25×10^{3}	241.06	8.68×10^{-4}	3.60×10^{-6}
^{242}Pu	8.17×10^{2}	242.06	5.68×10^{-4}	2.34×10^{-6}
^{129}I	3.13×10^{2}	129.00	2.17×10^{-4}	1.69×10^{-6}
^{234}U	3.06×10^{2}	234.04	2.13×10^{-4}	9.08×10^{-7}
^{230}Th	2.28×10^{-2}	230.03	1.58×10^{-8}	6.89×10^{-11}
^{233}U	1.40×10^{-2}	233.04	9.73×10^{-9}	4.17×10^{-11}
^{229}Th	6.37×10^{-6}	229.03	4.43×10^{-12}	1.93×10^{-14}
^{226}Ra	3.18×10^{-6}	226.03	2.21×10^{-12}	9.77×10^{-15}

[1]from Carter et al. (2012, Table C-1)

[2]from Sevougian et al. (2013, Table 1)

3.2 Engineered Barrier System

The description of EBS for the argillite reference case includes the following components:

- Waste Form
- Waste Package
- Repository Layout
- Backfill
- Seals

3.2.1 Waste Form

As described above, the reference case inventory is limited to PWR UNF waste. Each irradiated PWR assembly is assumed to contain 0.435 MTHM and 1.44×10^{6} g/MTHM of isotopes, with mass fractions of the selected radionuclides as listed in Table 1. This corresponds to a total mass of 6.27×10^{5} g of isotopes per PWR assembly. The PWR waste forms are assumed to be predominantly UO_2 with zircaloy cladding. UO_2 has a solid density of 10.97 g/cm^3 (Lide 1999, p. 4-94). Therefore, the solid volume of a PWR assembly can be approximated by $(6.27 \times 10^{5}$ g/assembly$)/(10.97 \times 10^{6}$ g/m$^3) = 0.057$ m^3.

Typical dimensions for unirradiated PWR assemblies are lengths of 111.8 to 178.3 in (2.84 – 4.53 m) and widths of 7.62 – 8.54 in (0.19 – 0.22 m) (Carter et al., 2012, Table A-1). Based on these dimensions, the total volume of a PWR assembly can range from about 0.10 – 0.22 m^3. The uranium loading (0.435 MTHM per assembly) is consistent with loadings, burn-ups, and enrichments of PWR assemblies listed in Carter et al. (2012, Table A-3).

The release of radionuclides from UNF includes a fast/instant release fraction (or IRF) – predominantly from radionuclides and fission gases located in the fuel and cladding gap, rod plenum regions (fission gases like Kr and Xe), and grain boundaries. Then a slower fraction – from radionuclides released from the UO_2 matrix through dissolution/conversion of the matrix. Sassani et al. (2012) describes the current

state of knowledge of IRF processes in irradiated used fuels, structural considerations (e.g., accessible and inaccessible grain boundaries; Figure 4), and IRF models, and distributions for the IRF of radionuclides. The IRF distributions are based on largely empirical correlations depending on the state of the fuel and cladding, burnup rates, and irradiation history. For PA sampling, Sassani et al. (2012) advances the IRF implementation in two sets of distributions: (a) triangular distributions representing minimum, maximum, and mean (apex) values for LWR used fuel with burnup at or below 50 GWd/MT, and (b) a process model has yet to be developed with functional parametrics. Table 3.2 1 of Sassani et al. (2012) provides model and values of IRF (% of radioelement inventory) for spent fuel pellets of various burnups, for a variety of environment conditions, and from various regions of the fuel pellet samples.

Information on radionuclide release from UNF in chemically-reducing environments for a granite repository is available from SKB (2010). The instant release fraction is different for different radionuclides. For ^{129}I, the instant release fraction has a mean of 0.025 and a standard deviation of 0.021 (SKB, 2010, Table 3-15). The fractional degradation rate of the UO_2 matrix has a best estimate of 10^{-7} yr^{-1}, a lower limit of 10^{-8} yr^{-1}, an upper limit of 10^{-6} yr^{-1}, and log-triangular distribution (SKB 2010, Table 3-21). The best estimate fractional degradation rate corresponds to a waste form half-life of 4,800,000 yrs. Although not considered in the salt reference case, HLW borosilicate glass waste forms typically have faster degradation rates.

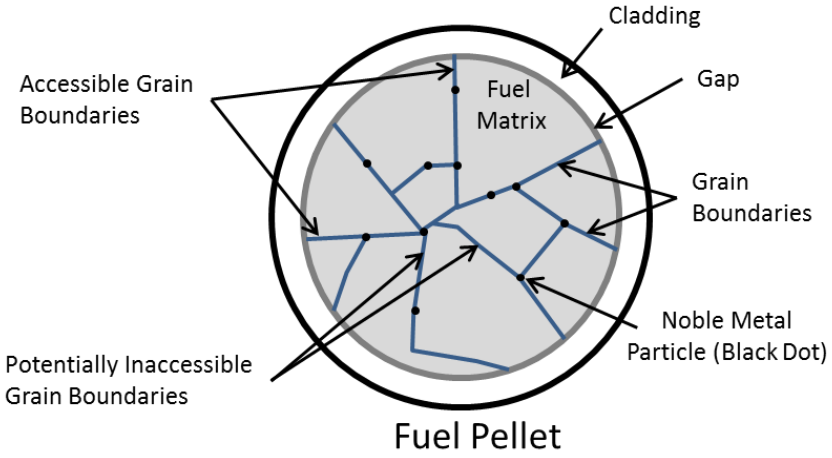

Figure 4. Schematic of a fuel pellet cross section showing the relative locations of radionuclide inventories for the gap, grain boundaries, fuel matrix, and noble metal particles. Also shown are the general locations of accessible grain boundaries and inaccessible grain boundaries (after Sassani et al. 2012).

3.2.2 Waste Package

The reference case considers the design for two types of waste package: the dual-purpose canister (DPC) that contains a high waste inventory of 32-PWR (Pressurized Water Reactor) fuel assemblies and the 12-PWR canister.

3.2.2.1 12-PWR Waste Package

The same as the salt reference case (Freeze et al. 2013), the argillite reference case also assumes waste packages consisting of a canister, containing 12 PWR UNF assemblies, and a disposal overpack. The 12-PWR waste package has length of 5.0 m and a diameter of 1.29 m (Hardin et al., 2012, Table 1.4-1). These outer dimensions include a 5.0 cm thick overpack. This overpack thickness is considered sufficient

to withstand general corrosion to ensure a retrievability period of 50 years (Sevougian et al. 2013, Section 2.2.3). More details of 12-PWR waste package are given in Freeze et al. (2013). Just as the assumption taken in Freeze et al. (2013), we will assume a burnup of 60 GWd/MT for 12 PWR as well.

3.2.2.2 32-PWR (DPC) Waste package

Hardin et al. (2013) discussed the characteristics of DPC while presenting the concept of direct disposal of DPC. The design capacity of DPC can accommodate 32-PWR assemblies or 68-BWR assemblies, and the average burnup for existing spent nuclear fuel (SNF) in dry storage is nominally 40 GWd/MT. We therefore assume a burnup of 40 GWd/MT for 32-PWR DPCs. The nominal dimensions of DPCs have a length of 5 m and a diameter of 1.74 m based on the HI-STAR 100 Multi-Purpose Canister (MPC-32) (Greene et al. 2013). The exterior dimensions of the MPC-32 should include an additional 5.0 cm thick overpack for a total outer diameter of about 1.79 m. It should be noted that the HI-STAR 100 design includes an overpack for storage with a wall thickness of 34.5 cm. Figure 5 shows a cross-section view of the MPC-32 for the HI-STAR 100 system.

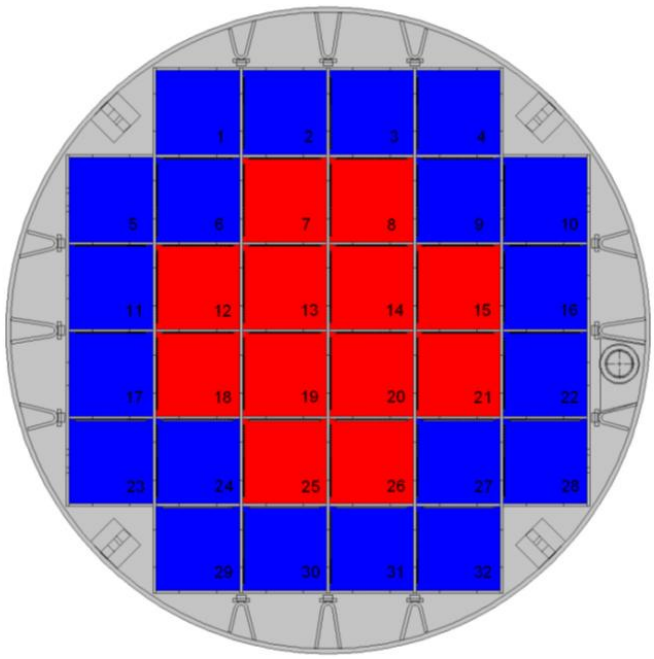

Figure 5. Cross-section view of the MPC-32 for the HI-STAR 100 system (after Greene et al. 2013).

3.2.3 Repository Layout

3.2.3.1 Layout for 12 PWR Waste Package

The repository layout must consider various operational, mechanical, and thermal design constraints. Liu et al. (2013) summarized the thermal constraints on EBS bentonite imposed in disposal concepts throughout the world for disposal in argillite and crystalline. A 100°C thermal limit is imposed unanimously in all these disposal concepts despite their differences in EBS design concepts. The same thermal limit was used when presenting the generic repository design concepts for clay (argillite) repository (e.g. Hardin et al., 2011; 2012). As a result, in order to address assumed thermal constraints imposed on the buffer materials and near field geologic media, waste packages that can accommodate 4-PWR or 9-BWR assemblies have been used in this concept (Hardin et al., 2011) and subsequently thermal analysis was done mostly for 4-PWR waste package for argillite repository. However, the basis for a

100°C thermal limit was not backed up by rigorous scientific studies (Liu et al., 2013). Reviews of the performance of bentonite backfill at temperatures exceeding 100°C (e.g., Wersin et al., 2007; Pusch et al., 2010), modeling (Liu et al., 2013; Zheng et al., 2014a), and experiment studies (e.g. Pusch et al., 2003; Caporuscio et al., 2012; Cheshire et al., 2013; Cheshire et al., 2014) of the mechanical and chemical changes at temperature up to 300°C showed little or moderate deterioration of bentonite. While further analyses of the THMC alteration of EBS bentonite and argillite at high temperatures are warranted, these modeling (e.g. Zheng et al., 2014a) and experimental (e.g. Cheshire et al., 2014) studies in the UFDC are suggestive that an argillite repository with EBS bentonite could sustain temperatures higher than a 100°C. Thermal analyses with the Disposal System Evaluation Framework (DSEF) are needed to determine the drift and waste package spacing under higher thermal loads, e.g., 150°C.

3.2.3.2 Layout for DPCs

The dimension of emplacement drifts for disposal DPC in argillite/shale rock is given in Hardin et al. (2013, Table 4-1). A drift 5 m high by 7 m wide or a circular cross-section with a diameter of 5.5 m was proposed in the report (Hardin et al., 2013). Greenberg et al. (2013) did a series of thermal analyses for 32-PWR waste packages with a burnup of 40 GWd/MT and with different drift and waste package spacings and ventilation times. In the reference case, we assume a drift spacing of 70 m, waste package spacing of 20 m, and ventilation time of 50 years. The temperature at the waste package surface and additional compliance points calculated by DSEF (Greenberg et al., 2013, case 500-11) are given in Table 2.

Table 2. The peak temperature at several compliance points for a argillite repository with a waste package of 32 PWR, 40 GWd/MT, drift spacing of 70 m, waste package spacing of 20 m, and ventilation time of 50 years (case 500-11 in Greenberg et al., 2013)

Location	Radius, m	Peak temperature, °C
Second compliance point	3.25	103.8
Peak rock	2.25	125.8
Liner inner surface	2.225	125.8
Backfill inner surface	1	233.9
Envelope inner surface	1	233.9
Waste package surface	1	233.9

3.2.4 Bentonite Backfill

The reference case considers two different waste-package designs: (1) a DPC that contains a larger waste inventory of 32-PWR fuel assemblies, and (2) a 12-PWR canister. In either design, an EBS consisting of backfill and liners is essential components. An engineered clay buffer backfill can be emplaced in a multi-layered configuration to optimize thermal, flow, and sorption properties of the buffer/backfill media. Figure 6 shows a double layer backfill configuration having two clay buffer materials for the 12-PWR canister. The choice of a double layer permits the use of two different clay buffer materials that can be tailored to optimize the barrier physical and chemical properties, while maintaining a low level of complexity in the EBS design. While the double layer backfill configuration can certainly be applied to the disposal of DPCs, a single layer backfill configuration (as shown in Figure 7) could also be another option. It may be operationally challenging to install a two-layer backfill to accommodate the relatively

large dimensions and substantial weight of a DPC. On the other hand, the high thermal load of a DPC would impose the partial sacrifice of the buffer layer closest to the waste package surface. The extent of such a "sacrificial layer" can be engineered with a tailored inner clay backfill layer as part of a double-layer system.

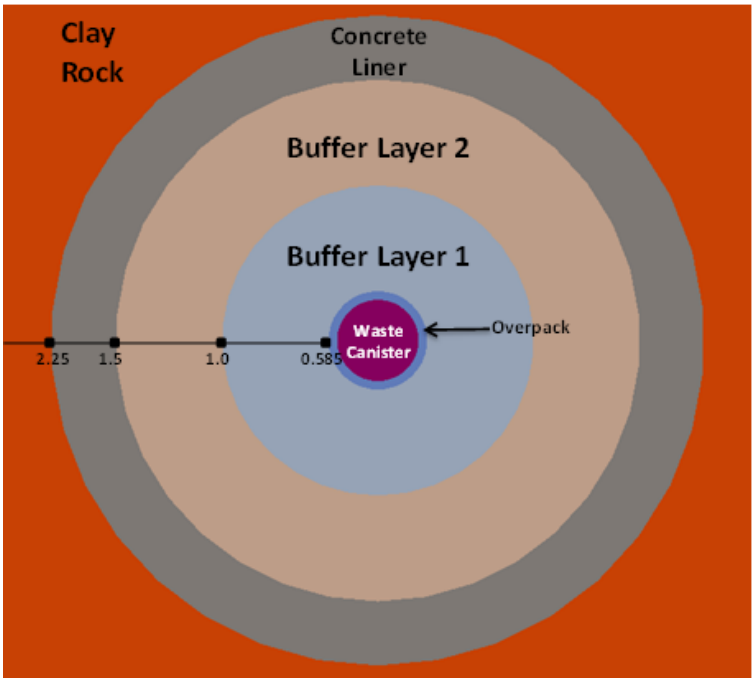

Figure 6. 2-D schematic diagram two-clay buffer layer EBS. Point values are radial distances in meters from the center of the waste canister (Jové Colón et al. 2013).

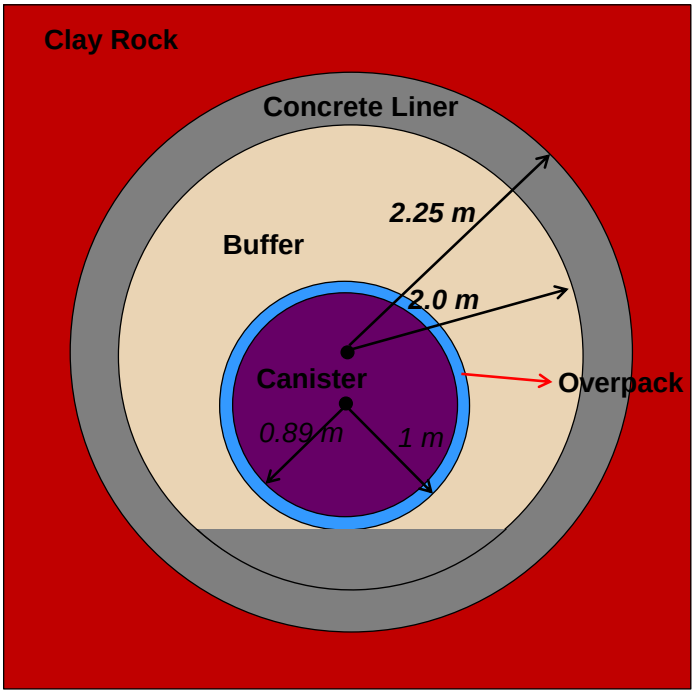

Figure 7. Geometry of a cross section of a drift for the disposal of DPC, largely based on Hardin et al (2013) and Greenberg et al. (2013).

3.2.4.1 Relevant Processes

Numerous modeling studies have been conducted by international research groups and by the UFDC. Some processes have long been identified as of great importance for the performance of a repository, such as diffusion and sorption. But the importance of some processes is not clear and requires more modeling and experimental studies. Here are the processes that are thought to be important and, therefore, have to be considered in the reference case:

- Heat transport by advection and conduction. An accurate prediction of the temperature profile in EBS is clearly important. The thermal limit in many countries (Hicks et al., 2009) is based on the temperature of the EBS.
- Fluid (water and vapor) flow by advection and diffusion. The hydrological condition is also obviously important, because they affect heat transport, mechanical changes, and chemical reactions in the EBS.
- Mechanical changes in the EBS, which are also important because they affect the long-term stability of the EBS and drift.
- Chemical reactions including mineral precipitation/dissolution, sorption, and cation exchange are very important, because they either directly control the migration of radionuclides or affect radionuclide transport indirectly through changes in the chemical conditions within the EBS. Cation exchange reactions also affect the volumes of the clay phase and thus its swelling properties.
- Interactions between the EBS and the canister materials, which have a significant impact on the redox environment and thus radionuclide solubility.

While the coupling between TH (e.g., heat transport by the advection of water), TC (e.g., change of mineral solubility with temperature), TM (e.g., thermal expansion and pressurization) and HC (e.g., solute transport by advection) are known to be important, recent modeling work sheds light on the importance of HM (such as swelling due to moisture change) and MC (e.g. change in swelling pressure due to pore-water chemistry changes) couplings. Coupled THM models have been developed in Rutqvist et al. (2009, 2011, 2014a, 2014b). The results from the model developed in Rutqvist et al. (2014b) show that it takes about 2780 years to fully saturate the EBS bentonite if the interaction between micro- and macro-structures is considered. This is much longer than the saturation time for the EBS predicted with single-structure models. Coupled THMC models have also been developed (Liu et al. 2013; Zheng et al. 2014a) to evaluate the impact of chemical processes on mechanical behavior, specifically the effect of illitization, pore-water chemistry changes, and cation exchange on the swelling of EBS bentonite. Liu et al. (2013) showed that chemical changes result in a decrease in swelling pressure of 0.2–0.3 MPa (about 20–30% of the swelling capacity) for Kunigel-VI bentonite (JNC 2000). In one extreme case, Kunigel-VI bentonite could loss up to 70% of its swelling capacity, which suggests that MC coupling is important for Kunigel-VI bentonite. Zheng et al. (2014a) conducted model studies which consider FEBEX bentonite (ENRESA, 2000) as the EBS buffer/backfill material. Model results showed only a moderate decrease in swelling stress of about 0.08 MPa, accounting for just 2% of the swelling capacity of FEBEX bentonite. The possible reasons for FEBEX bentonite suffering less swelling pressure loss than Kunigel-VI bentonite are as follows: (a) less illitization is predicted for FEBEX bentonite, and (b) FEBEX bentonite has much higher swelling capacity (5–8 MPa) than Kunigel-VI bentonite (around 1MPa). The tentative conclusion from current THMC models is that MC coupling does not necessarily need to be included in a performance assessment model. However, before making the determination that MC coupling may be neglected, coupled THMC modeling is warranted when site-specific data are available. The bentonite properties that need to be specified to address these processes are given the following section.

3.2.4.2 Thermal, Hydrological and Mechanical Properties

The basic material in the backfill is typically bentonite which is an impure clay consisting mostly of smectite (montmorillonite), along with small amounts of other minerals such as quartz and feldspar. In some disposal concepts (ENRESA 2000; SKB 2006), the backfill contains bentonite exclusively, but mixtures of bentonite with graphite or silica phases (e.g., quartz) have also been considered in some disposal concepts to enhance thermal conductivity (e.g., JNC 2000). In this report, we focus on the properties of two widely studied bentonites; the properties for mixtures of bentonite with other materials are not discussed here.

Table 3 lists typical thermal, hydrological and mechanical parameters for two bentonites that have been studied as the backfill material for nuclear waste disposal: the FEBEX (ENRESA 2000) and MX-80 bentonite (SKB 2006). Thermal, hydrological and mechanical properties for bentonite vary a great deal with the degree of compaction (dry density). Those properties listed in Table 3 are for the dry density range that is widely used in tests of different scales and are considered candidates for use in a future repository. For example, a dry density of around 1650 kg/m^3 for FEBEX bentonite bricks has been used in the Mockup and In Situ test (ENRESA 2000) and it is also the design used in the Spanish reference concept for high level nuclear waste disposal (ENRESA 2000).

Properties (see Table 3) for FEBEX and MX-80 bentonite are largely from ENRESA (2000) and SKB (2006), respectively, but some are taken from various other sources as noted below.

Saturated permeability for FEBEX bentonite is typically around 2–3×10^{-21} m^2, but a summary from various sources (ENRESA 2000; Börgesson and Hernelind 2005; Zheng et al. 2011a) leads to a larger range of permeabilities.

The relative permeability curve for FEBEX bentonite is typically given as:

$$K_{rl} = S^n \tag{1}$$

where K_{rl} is the relative permeability, S is the water saturation, and n is a constant. The exponent n ranges from 3 to 4.5 (ENRESA 2000), but most models (Zheng et al. 2011a; Sánchez et al. 2012) have used 3. The relative permeability curve for MX-80 bentonite is the same as in equation (1), with n ranging from 2 to 4 (Hökmark 2004).

Typically the van Genuchten (van Genuchten 1980) function is used for water retention curve, which expresses the capillary pressure, s, as a function of water saturation, S.

$$S_w = S_r + (S_m - S_r)\left[1 + \left(\frac{s}{P_0}\right)^{\frac{1}{1-\lambda}}\right]^{-\lambda} \tag{2}$$

where S_r and S_m are the residual and maximum degree of water saturation, P_0 is the material property that represents capillary strength, and λ is m in van Genuchten's notation, which represents the effects of the pore-size distribution. ENRESA (2000) lists a quite large range of λ and $P_{0,}$ but in some modeling works (Zheng et al. 2011a; Sánchez et al. 2012), λ is 0.18 and P_0 is 2×10^7 Pa; Villar et al. (2008) used the same value of λ but a slightly different value for P_0 (2.8×10^7 Pa). The parameters λ and P_0 for MX-80 bentonite are from Hökmark (2004). The specific heat capacity for MX-80 bentonite is from Man and Martino (2009).

Table 3. Thermal, hydrological and mechanical parameters for two bentonites.

Parameter	FEBEX bentonite	MX-80 bentonite
Grain density [kg/m^3]	2700	2700
Dry density [kg/m^3]	1650-1700	1650-1700
Porosity ϕ	0.41	0.41
Thermal conductivity [W/m ^{o}C] dry/wet	0.57/1.28	0.3/1.3
Saturated permeability [m^2]	1.75×10^{-21} - 8×10^{-21}	2.0×10^{-21}
Relative permeability, k_{rl}	$K_{rl} = S^3$	$K_{rl} = S^3$
van Genuchten P_0 (Pa)	2×10^7 to 1×10^8	0.9×10^7 to 2×10^7
van Genuchten *m* (or λ)	0.18-0.475	0.4-0.45
Compressibility, β [1/Pa]	3.2×10^{-9}	3.2×10^{-9}
Thermal expansion coeff., [1/^{o}C]	1.0×10^{-5}	1.0×10^{-5}
Dry specific heat, [J/kg ^{o}C]	767-939	800
Tortuosity for vapor phase	$\phi^{1/3}S_g^{10/3}$	$\phi^{1/3}S_g^{10/3}$
Swelling pressure (MPa)	5-10	7.5-8

3.2.4.3 Chemical Properties

The chemical properties of the buffer layer are critical for the performance of a repository. First, these properties significantly affect the chemical environment in which canisters or overpack react with incoming formation water. Second, the buffer layer serves as the first barrier for retarding radionuclide migration, the effectiveness of that retardation is highly sensitive to the chemical conditions in the buffer. The most relevant chemical properties of bentonite buffer are the initial-state mineral and aqueous compositions.

Mineralogical Composition

The most prominent mineral in bentonite backfill is smectite clay, which typically accounts for 40 to95% of the total mass of bentonite. Table 4 lists the mineral compositions of FEBEX and MX-80 bentonites. In addition to smectite, quartz, K-feldspar, and oxides are common accessory minerals. Highly soluble minerals such as calcite and gypsum could also be present. These minerals could have a significant impact on the pore-water chemistry during the hydration of EBS bentonite.

Table 4. Mass fraction (%) of minerals for FEBEX (ENRESA 2000; Fernández et al. 2004) and MX-80 bentonite (Börgesson et al. 2006).

Mineral	FEBEX bentonite	MX-80 bentonite
Calcite	trace	0
Dolomite	0.0	0
Illite	0.0	1
Kaolinite	0.0	0
Smectite	92 ± 3	87
Chlorite	0.8	0
Quartz	2 ± 1	3
K-Feldspar	trace	3
Siderite	0.0	0
Ankerite	0.0	0
Cristobalite	2 ± 1	0
Plagioclase	2 ± 1	0
pyrite	0.02	0.25
Mica		4
Gypsum	0.14	0.7

Pore-water *Chemistry at the Initial State*

Pore-water chemistry at the initial state of bentonite backfill is very important, because it affects the chemical environment in which the radionuclides migrate. The initial state of bentonite backfill for the repository conditions is typically characterized by the dry density and water content, or solid/liquid ratio. For example, FEBEX bentonite blocks have an initial gravimetric water content of 13.5–14% (ENRESA 2000), which is about 56% in terms of volumetric water content (Zheng et al. 2011a). However, as mentioned in Bradbury and Baeyens (2003a), obtaining the pore-water chemistry of compacted bentonite is not a straightforward task, and therefore there is considerable uncertainty is associated with the concentrations of ions in the pore-water. Major uncertainties are as follows:

1. The concentration of ions for the initial state of compact bentonite cannot be measured directly; therefore indirect measurement methods have to be used. Squeezing and aqueous extract are the most commonly used methods. Squeezing is a straight forward method — pore-water is squeezed out and concentrations are measured. However, squeezing does not allow extracting of pore-water from clay samples with gravimetric water contents less than 20% (Fernández et al. 2001, 2004), which means that squeezing cannot be done for FEBEX bentonite blocks, which initially have a water content 14% (ENRESA 2000). In an aqueous extract test, a crushed sample is placed in contact with water at a low solid/liquid ratio (ranging from 1:16 to 1:1). After establishing equilibrium, the solid phase is separated and the liquid phase is analyzed (Fernández et al. 2001). Because of the low water content (high solid/liquid ratio as well), the pore-water chemistry at the initial state can only be measured indirectly by squeezing conducted at higher water content or aqueous extract. But both methods introduce artifacts and alter the geochemical system, resulting geochemical modeling needing be employed to retrieve the aqueous ion concentrations at low water content (Zheng et al. 2008). Any uncertainties associated with the geochemical models affect concentration levels at low water content (the water content at the initial state).
2. It is generally agreed that there are two types of pore-water in compacted bentonite: (1) external or intergranular water that resides in large pores, and (2) interlayer water which stays in the interlayer spaces between the smectite clay layers (e.g., Bradbury and Baeyens 2003a). External

water can be viewed as two types: (1) bulk or "free" water and (2) diffuse double layer (DDL) water. Typically the "pore-water" refers to the free water, whose concentrations are for the ions in bulk aqueous solution. However, the interface between bulk pore-water and double layer water is vague and changes with saturation (or solid/liquid ratio) and solution ionic strength.

3. Compacted bentonite blocks are typically fabricated by adding a small amount of water to dry bentonite power. Sometimes deionized water is used, and sometimes the water from the potential host formation is used, which affects the pore-water chemistry.

Table 5 lists the concentration of major ions in compacted MX-80 and FEBEX bentonites as examples. The pore-water for FEBEX bentonite is calculated from measured concentrations at different solid/liquid ratios with bentonite being mixed with granite water from the Grimsel test site (ENRESA 2000). Pore-water for MX-80 bentonite is calculated from data obtained by mixing MX-80 bentonite powder with Opalinus Clay pore-water (Curtis and Wersin 2002).

Table 5. Pore-water composition of FEBEX bentonite (Fernández et al. 2001) and MX-80 bentonite (Curtis and Wersin 2002).

Species	MX-80 Bentonite	FEBEX Bentonite
pH	7.25	7.72
Cl	1.91E-1	1.60E-01
SO_4^{-2}	6.16E-2	3.20E-02
HCO_3^-	2.83E-03	4.1E-04
Ca^{+2}	1.32E-02	2.2E-02
Mg^{+2}	7.64E-03	2.3E-02
Na^+	2.74E-01	1.3E-01
K^+	1.55E-03	1.7E-03
Fe^{+2}	4.33E-05	NR*
SiO_2(aq)	1.80E-04	1.1E-04
AlO_2^-	1.92E-08	NR*

*not reported

Sorption Properties

Cation exchange capacity (CEC) is usually needed for reactive transport modeling of a repository system: it generally represents the sorption capacity of bentonite. FEBEX bentonite has a CEC of ~102 meq/100 g (ENRESA 2000; Fernandez et al. 2001) and MX-80 bentonite has a CEC of ~78.7 meq/100 g (Bradbury and Baeyens 2002). Table 6 shows the cation occupancies of the exchangeable sites.

Table 6. The CEC and exchangeable cations for FEBEX bentonite (Fernández et al. 2001) and MX-80 bentonite (Bradbury and Baeyens 2002).

Cations (meq/100 g)	MX-80 Bentonite	FEBEX Bentonite
Ca^{+2}	6.6	34.6
Mg^{+2}	4.0	34.0
Na^+	66.8	31.1
K^+	1.3	1.94
CEC (meq/100 g)	78.7	102

The radionuclide sorption properties of the clay material are represented in the form of K_d (distribution coefficients) or retardation factor, R_d. K_d is defined as the ratio of the sorbed radionuclide mass per unit mass of solid divided by the radionuclide solution mass concentration. R_d is defined as:

$$R_d = 1 + \frac{\rho_d}{\theta} K_d \quad (3)$$

where ρ_d is the dry bulk density of the soil and θ is the volumetric water content.

The K_d approach and its variants have been widely adopted in transport calculations and have been calibrated to capture dependencies, such as aqueous phase and bulk rock chemistry. K_d values for various radionuclides have been determined for various types of materials. Current UFD work (experimental and modeling) is under way to assess diffusion data for U and other radionuclides in clay material. Reactive diffusion through clay is also part of this effort to mechanistically represent the effect of compacted porous clay on diffusive fluxes, particularly for charged species. Sorption data (expressed as a retardation factor, R_d) for MX-80 bentonite were tabulated in Bradbury and Baeyens (2003b), with a subset of those tables shown in Table 7. A critical review of K_d for several bentonites and argillites are given in Miller and Wang (2012).

Table 7. In situ retardation factor R_d value (m^3/kg) for the MX-80 bentonite at pH = 7.2 (Bradbury and Baeyens 2003b)

Species	Retardation factor	Species	Retardation factor
Cs(I)	0.12	Ra(II)	0.0021
Ce(III)	4.7	Ac(III)	26.8
PM(III)	4.7	Th(IV)	63
Sm(III)	4.7	Pa(V)	5
Eu(III)	4.7	U(IV)	49.1
Ho(III)	4.7	Np(IV)	63
Hf(IV)	81	Pu(III)	26.8
Pb(II)	7.9	Am(III)	26.8
Po(IV)	0.068	Cm(III)	26.8

Diffusion coefficients are important parameters that control the migration of radionuclides. Although the diffusion coefficient for major cations such as Na and trace elements such Sr and Cs have been widely studied—for example, García-Gutiérrez et al. (2001) for FEBEX bentonite and Ochs et al. (2001) for MX-80 bentonite—the diffusion coefficients for radionuclides are not widely reported. Table 8 lists the effective diffusion coefficients of several radionuclides for MX-80 bentonite (Brandberg and Skagius 1991).

Table 8. Effective diffusion coefficient for some elements for MX-80 (Brandberg and Skagius 1991).

Species	Effective diffusion coefficient (m^2/s)
C-14	10^{-10}
I-129	2×10^{-12}
Sr-90	2×10^{-8}
Cs-137	2×10^{-9}
Na-22	2×10^{-9}
Pu-238	10^{-10}
Am-234	10^{-10}

Radionuclide Solubilities

Radionuclide solubility must be considered as a key limiting mechanism to arrest species mobility. These solubilities can be estimated through chemical equilibrium calculations using existing thermodynamic data. Some limitations exist with regard to temperature and the effects of ionic strength. However, such

calculations have been performed and embedded in PA calculations with uncertainty bounds to address some of these limitations. Current efforts directed at describing used fuel interactions and the effects of radiolytic phenomena will provide a comprehensive analysis of source term releases (Buck et al. 2013).

Bernot (2005) provides an evaluation of radionuclide solubilities for implementation into PA. Recent efforts in thermodynamic database development, along with tools for computing solution-mineral equilibria, are being assessed for a more rigorous computation of solubility limits. Such type of evaluation could be used to bound solubilities of actinides like plutonium, neptunium, uranium, thorium, americium, actinium, and protactinium.

3.2.5 Concrete Liner

Ground support for the drift is generally needed, especially for the disposal of DPCs. Hardin et al. (2013) mentioned that steel sets or shotcrete could be used, with the latter probably being more economically viable. Currently, for the reference case, a 25 cm thick shotcrete layer (Figure 7) is considered. Similar to the bentonite backfill, shotcrete undergoes simultaneous THMC alterations. Those processes that are relevant for the bentonite backfill are also important for the concrete liner. Because coupled THMC models for shotcrete were not found in the literature, the importance of some coupled processes such as HM and MC couplings cannot be evaluated. HM and MC presumably might not be too important. For example, moisture-induced stress changes, the predominant HM coupling, might not be important because concrete is much more rigid than bentonite; chemically-induced stress change, a typical MC coupling, would not be significant unless concrete undergoes significant chemical changes. However, coupled model should be done before deciding to neglect HM and MC couplings. Because a concrete liner is emplaced between the bentonite backfill and argillite host rock, concrete/bentonite and concrete/argillite interactions are potentially important. Experimental and modeling studies of concrete/bentonite interaction are reviewed in Gaucher and Blanc (2006). Kosakowski and Berner (2013), Gaboreau et al. (2012), and De Windt et al. (2008) provide modeling studies of concrete/argillite interactions. The parameters needed to describe those processes are given below.

3.2.5.1 Thermal, Hydrological and Mechanical Properties

Shotcrete has been used in the Full-Scale Emplacement Experiment (FE) at the Mont Terri URL, Switzerland (Vietor 2012) and models for scoping calculations and benchmarking have been developed in Houseworth et al. (2013). Table 9 lists the thermal and hydrological parameters for shotcrete used in these models. The relative permeability and retention curve for shotcrete are described by the van Genuchten relationship, with formats shown in Equations (4) and (5). The parameters for Equations (4) and (5) are given in Table 9:

The water relative permeability in the shotcrete is given by:

$$k_{rw}(S_w) = \left(\frac{S_w - S_r}{S_m - S_r}\right)^{1/2} \left[1 - \left\{1 - \left(\frac{S_w - S_r}{S_m - S_r}\right)^{1/m}\right\}^{m}\right]^2 \quad (4)$$

Capillary pressure in the shotcrete is given by:

$$\psi(S_w) = \frac{1}{\alpha}\left\{\left(\frac{S_w - S_r}{S_m - S_r}\right)^{-1/m} - 1\right\}^{1-m} \quad (5)$$

where $\frac{1}{\alpha}$ is equivalent to P_0 in Equation (2).

Table 9. Thermal and hydrological parameters for shotcrete (Houseworth et al. 2013).

Parameters	Shotcrete
Solids density (kg/m^3)	2700.
Porosity	0.15
Permeability (m^2)	3.5 x 10^{-21}
Thermal conductivity (saturated) (W/m)	1.7
Specific heat (solids)	800.
Thermal conductivity (desaturated) (W/m)	1.06
Tortuosity	1.
Water relative permeability parameter *m*, (Equation (4))	0.52
Water relative permeability residual saturation, S_r (Equation (4))	0.0071
Water relative permeability maximum saturation, S_m (Equation (4))	1.
Capillary pressure parameter, α (Pa^{-1}) (Equation (5))	9.091 x 10^{-8}
Capillary pressure parameter, *m*, (Equation (5))	0.29
Capillary pressure residual saturation, S_r (Equation (5))	0.0071
Capillary pressure maximum saturation, S_r (Equation (5))	1.
Vapor and air diffusion coefficients (D in Equation (6)) (m^2/s)	2.68 x 10^{-5}
Vapor and air diffusion temperature exponents, (n in Equation (6))	2.3

The vapor and air diffusion coefficients are both given by, D_g^w, which is modeled as a function of temperature and gas-phase saturation using the following relationship,

$$D_g^w = \tau S_g D \frac{P_{g0}\left(273.15+T\right)^n}{P_g\left(273.15\right)^n} \tag{6}$$

where P_g is the gas phase pressure, T is the temperature in Celsius, P_{g0} is the gas-phase pressure at a temperature of zero Celsius, τ is the tortuosity, S_g is the gas saturation, and D is the diffusion coefficient at a temperature of zero Celsius, and n is an empirical coefficient.

3.2.5.2 Chemical Properties

Table 10. Mineralogical composition of concrete De Windt et al. (2008).

Mineral	Shotcrete
Calcite (aggregate)	66.5
CSH 1.8	23
Ettringite	1.5
Hydrotalcite	0.5
Monosulfoaluminate	1.5
Portlandite	0.8

The properties of concrete vary according to the locations where the cement is fabricated. De Windt et al. (2008) modeled reactive transport at the concrete/argillite interface. Table 10 lists the mineralogical composition of concrete used in their model. The pore-water composition of concrete is not widely reported, but with the knowledge of mineral composition, pore-water composition can be established via geochemical modeling. An example of concrete pore composition calculated by equilibrating unhydrated cements with water is given in Kosakowski and Berner (2013). A thermodynamic database for clay and

cementitious materials has been compiled in a previous report (Jové Colón et al, 2011) along with modeling tool development of C-S-H solid solution and computation of equilibrium aqueous species concentrations (Jové Colón et al, 2012).

Sorption is also an important process, one that controls the migration of radionuclides through concrete. McKinley and Scholits (1993) compiled and compared different sorption databases for cements, which are listed in Table 11.

Table 11. The distribution coefficient (K_d) for several cements McKinley and Scholits (1993).

Database:	NAGRA	DOE, U.K.	Nirex	TVO	SKB	GSF
Sorbing material:	Cement	Cement	Cement	Cement	Cement	Cement (fresh)
Reference:	[1]	[2]	[3]	[4]	[5]	[6]
Cs	0.002	0.0001	0.005	0.1	0.001	0.0004
Sr	0.002	0.005	0.002	0.005	0.001	0.0004
C_i	5	10	6		1	0.0004
I	0.03	0.001	0.0001	0.005	0.003	0.0004
Se		0.005	0.0005			0.0004
Ni	1	0.005	0.05	3	0.5	0.0004
Pd	0.2		0.01			0.0004
Sn	0.2	0.005	0.01			0.0004
Zr	1	0.005	0.1			1
Tc	0.1	0.001	0.1	0.2	0.1	0.0004
Am	5	5	5	0.5	1	1
Np	5	1	5			1
Pu	5	8	5	1	1	1
Th	5	0.2	5			1
U	5	0.2	1			1

References: [1] = Allard (1985); [2] = Nacarrow et al. (1988); [3] = Ewart et al. (1988); [4] = Vieno and Nordman (1991); [5] = Wiborgh and Lindgreen (1987); [6] = Buhmann et al. (1991).

3.3 Seals

Seals comprise the isolation system emplaced in deep repository structures—such as shaft/tunnel/disposal gallery accesses and drift linings and/or support assemblies—to limit radionuclide mobility and fluid flow beyond the confines of the near-field environment. The shaft seal system is designed to limit access of formation water into the repository and disposal galleries. Conversely, it is also designed to restrict the outflow of contaminated fluids from the repository.

Extensive work conducted at the WIPP repository provides the basis for the evaluation of the expected performance depending on the seal configuration and materials to be considered. The design guidance items for a shaft seal system are given by Hansen et al. (2010):

- Limit waste constituents reaching regulatory boundaries
- Restrict formation water flow through the sealing system
- Use materials possessing mechanical and chemical compatibility
- Protect against structural failure of system components

• Limit subsidence and prevent accidental entry
• Utilize available construction methods and materials.

Seal materials include cement and clay that are consistent with shaft sealing material specifications and the repository makeup. In general, small amounts of groundwater (if any) are expected to percolate into the repository even with distal or proximal aquifers. Although cement and bentonite clay are regarded as stable seal materials, potential processes such as thermally-induced phase transformations and interactions with intrinsic or extrinsic fluids may cause degradation. However, significant degradation of this type is not expected to occur in a clay/shale repository, given the expected level of isolation. Another aspect of seals is its close relationship to the excavated disturbed zone (EDZ) as described by Bianchi et al. (2013). Permeability ranges for seals can be obtained from existing literature sources for cement and clay materials. The properties of cement and bentonite are given above in Sections 2.1 and 2.2.

3.4 Natural Barrier System

The natural barrier system (NBS) for the reference case includes the unaltered host rock and the excavation damaged zone (EDZ) around the tunnels and access shafts of the repository. The host rock is represented by an argillaceous formation characterized by low permeability, high retention capacity for radionuclides, and potential self-sealing of fractures. Geological formations with similar properties are currently under consideration for disposal of HLW by several countries such as France (argillite), Belgium (plastic clay), and Switzerland (claystone). Argillaceous or clay-rich formations can have a wide range of lithologies in terms of degree of consolidation, textural parameters (e.g., presence of lamination), and mineralogical composition (i.e., type of clay minerals, percentage of carbonate or quartz particles). Moreover, the term "clay" is often ambiguous, since it can be used to refer to a group of minerals (clay minerals), rock fragments rich in clay minerals, or sediment grains smaller than fine silt (< 2 μm). Because of the wide range of clay-rich formations in the United States, and the fact that a specific site has not been yet identified, the generic term *argillaceous formation* is used to describe the host rock in the reference case. This term indicates a generic sedimentary formation with a lithological composition of at least 50% clay. More specific details on the argillaceous formation considered in the reference case are presented in the next section.

3.4.1 Relevant Processes

Those processes relevant to the performance of EBS bentonite are also important for the argillite host rock, including heat transport by advection and conduction, water flow by advection, vapor flow by advection and diffusion, mechanical changes, and chemical reactions. Vapor flow by diffusion is of particular importance for argillite in the short term. Argillite near the concrete/argillite might become unsaturated for a short period for the disposal of 12-PWR canisters whereas argillite undergoes a desaturation during ventilation for the disposal of DPCs (Zheng et al. 2014c). Concrete/argillite interactions could have significant impact on the migration of the radionuclides because minerals precipitation in concrete might cause pore clogging (Gaboreau, et al. 2012).

Coupled THM models for argillite have been developed in Rutqvist et al. (2014a) and coupled the THMC models have also been developed (Liu et al. 2013; Zheng et al. 2014a, 2014b). Because of significant increases in stress due to thermal pressurization (Rutqvist et al. 2014a), the stress change due to illitization caused by MC coupling (Liu et al. 2013; Zheng et al. 2014a) seems not to be very important. However, the effect of illitization on the sorption capacity of argillite still requires further study. MC coupling is therefore not deemed indispensible in the performance assessment model. However, when site-specific data are available, the use of a coupled THMC model is warranted before deciding to neglect MC coupling.

3.4.2 Properties of the Argillaceous Host Formation

For the reference case, the stratigraphic setting and hydrogeological properties of a generic argillaceous formation are made consistent with the characteristics of argillaceous units in four major shale provinces in the United States based on the classification of Gonzales and Johnson (1984): Eastern Interior, Great Plains, Rocky Mountains, and Colorado Plateau. These provinces were chosen because of the higher number of units with potential for HLW storage (Table 1-1 in Hansen et al. 2010). Figure 8 shows the areal distribution of shale in the USA along with depth to top mapping of formation units. In collecting data from several potential units, we also considered the recommendations of Hansen et al. (2010) and Shurr (1977):

- Formation thickness: Formation thickness should be at a minimum 150 meters. Lesser values have been proposed (75 meters) but larger thicknesses are desirable depending on formation stratigraphic uniformity.
- Depth: The repository horizon should be at a depth between 300 to 900 meters. A depth of ~600 meters is considered generic disposal concepts. The report by Perry et al (2014a) provides an analysis of shale formation depths and thicknesses distributed along continental USA.
- Low hydraulic conductivity: Shale media is highly desirable for its very low permeability with small values in the order of 10^{-14} – 10^{-22} m^2.
- Areal coverage: Widespread distributions of sedimentary basins in the continental USA contain thick shale sequences extending hundreds of kilometers. Gonzales and Johnson (1985) and more recently Perry et al. (2014a) provide a comprehensive description of shale distribution in the USA.
- Self-healing: A key property of shale is plasticity (along with swelling) allowing for healing or self-sealing (used here interchangeably) of fractures as a result of burial processes or during excavation activities. Self-healing leads to reduction to hydraulic conductivity of fracture and can occur through chemo-mechanical (swelling), chemical (fracture filling and mineral precipitation), and mechanical closure of fracture through rock deformation (Mazurek et al. 2003).
- Mineralogy: Shale formations can have variable mineralogy and organic content. The desirable mixed-clay fraction (illite/smectite) should exceed 85% where the remainder is usually as assemblage of accessory minerals such as quartz, Fe oxides, pyrite, and feldspar.
- Stratigraphic and structural uniformity (bedding and faulting): Uniform stratigraphy (e.g., lack of sandstone lenses, and allocthonous materials) with low bedding angle or flat-lying sequences and marginal thick sedimentary layering within the repository horizon. Minimal structural geologic features such as folding, faulting, and joint/fractures is desirable within the extent of the repository footprint.
- Hydrogeochemistry: The hydrochemistry of deep-seated clay-bearing is often represented by reduced aqueous fluids with bulk chemistries enriched in Na-Ca-Cl-SO_4 and often saline. Salinity tends to increase with depth due increase fluid isolation. Therefore, mixing with more diluted waters from overlying or much shallower formations is usually not observed.
- Tectonic and/or seismogenic stability: Preference is given to areas that are seismically quiet, devoid of active faults or far from major tectonic lineaments.

- Borehole activity: Oil and gas drilling targets for hydrocarbon resource exploration and production in shale is unwanted, particularly in the exploitation of unconventional shale reservoirs.

In the Eastern Interior Province, the characteristics of the Upper Ordovician Black River Group and Middle Ordovician Trenton Group of the Michigan Basin were considered (Clark et al. 2013; Beauheim et al. 2014) . In the Great Plains Province, most of the data analyzed refers to the Pierre Shale (Neuzil 1986; 1993; Bredehoeft et al. 1983; Olgaard et al. 1995; Smith et al. 2013).

Based on this information, the reference case assumes a depth for the top of the argillite host formation of 450 m (with a range of ~300 m to 900 m), a thickness of 150 m (with a range of ~75 m to 300 m), and an extent of 300 km x 300 km (with a range of of ~100 km × 100 km to 500 km × 500 km). There are several locations in the Eastern Interior, Great Plains, Rocky Mountains, and Colorado Plateau shale provinces that have argillaceous formations with these ranges of depth, thickness, and areal extent, such that they can be targeted for HLW disposal. It is also assumed that the argillaceous formation is bounded at the top and at the bottom by two geological units with permeability 4 to 5 orders of magnitude higher than the argillaceous host rock. The lithology of these surrounding units is not specified at this stage, but will be specified when a site will be selected.

As for the structural and stratigraphic setting, the values assumed for the hydrogeological properties of the argillaceous host formation in the reference case are based on available data from argillaceous formations in the U.S. (Table 12). The permeability of the unaltered argillaceous rock is assumed equal to 5×10^{-20} m^2 (with a range of 1×10^{-19} m^2 to 1×10^{-21} m^2). This value is also consistent with the range of permeability values measured in argillaceous formations currently under investigation as potential host rock for HLW disposal, such as the Callovo-Oxfordian Argillites (e.g., ANDRA 2005, Armand et al. 2013), and the Opalinus Clay (e.g., NAGRA 2002; Croisé et al. 2004). The same value was also adopted by Bianchi et al. (2013; 2014). The total porosity is assumed equal to 0.15 (with a range of 0.1 – 0.4), while the accessible porosity—that is, the fraction of pore space that actually accessible to diffusion—is assumed equal to 0.08 (with a range of 0.04 to 0.1).

3.4.3 Hydraulic Conditions in the Argillaceous Formation

The reference case formation is assumed saturated with a specific storativity of 1.0×10^{-5} m^{-1} (with a range of 8.0×10^{-6} m^{-1} to 4.0×10^{-5} m^{-1}). A vertical upward hydraulic gradient equal to 1 m/m is assumed. At this stage, the hydraulic head distribution in the reference case is assumed at equilibrium relative to the hydraulic heads in the overlying and underlying formations with higher permeability. However, an anomalous head distribution within the host formation is expected since this phenomenon is typically observed in several argillaceous formations. For example, hydraulic head measurements in the Callovo-Oxfordian argillite at Bure, France, revealed overpressures between 20 to 40 meters water column equivalent relative to the upper and lower surrounding formations (ANDRA 2005). Similarly, the Opalinus Clay near Benken, Switzerland (NAGRA 2002) is overpressurized. In the U.S., the Middle Ordovician Trenton Group in the Michigan Basin is significantly underpressurized (Beauheim et al. 2014). Hydraulic head data for the Pierre Shale in South Dakota also provide evidence of underpressurized conditions with head values as much as 125 m below hydrostatic level (Neuzil, 1993; Figure 9). As shown recently by Bianchi et al. (2014), pressure anomalies within the host argillaceous formation can have an impact on radionuclide transport from the repository toward the biosphere. In particular, inward flow caused by negative pressure anomalies in the host rock can delay radionuclide transport enhancing the ability of the geological barrier to contain the radioactive waste (Neuzil, 2013). Conversely, local high gradients, owing to the presence of overpressures, can speed up the transport process. Pressure conditions within the host rock will be thoroughly assessed once more specific details of the argillaceous host formation become available.

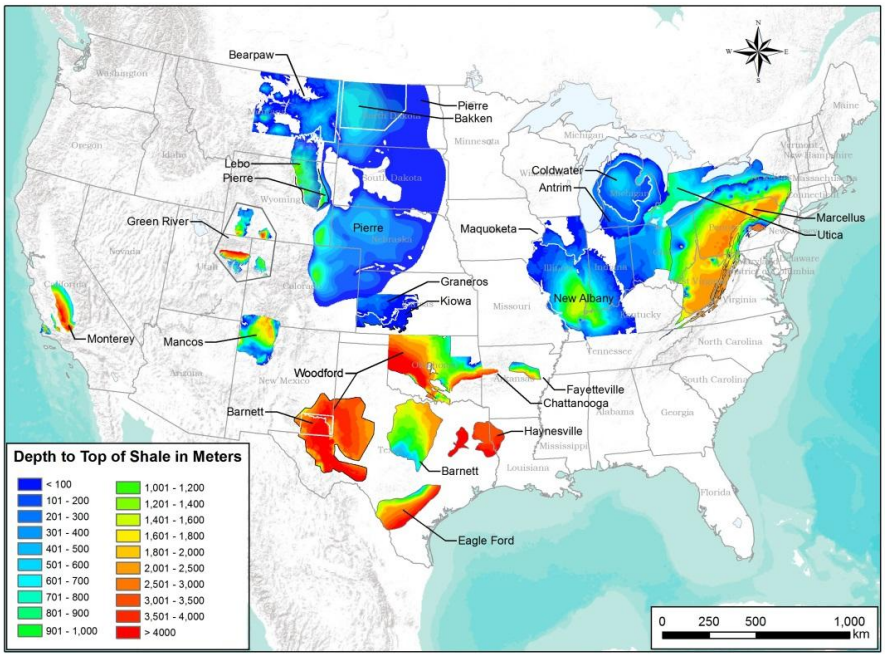

Figure 8. Distribution of the clay-rich formations in the USA along with depth to top mapping (updated from Perry (2014a))

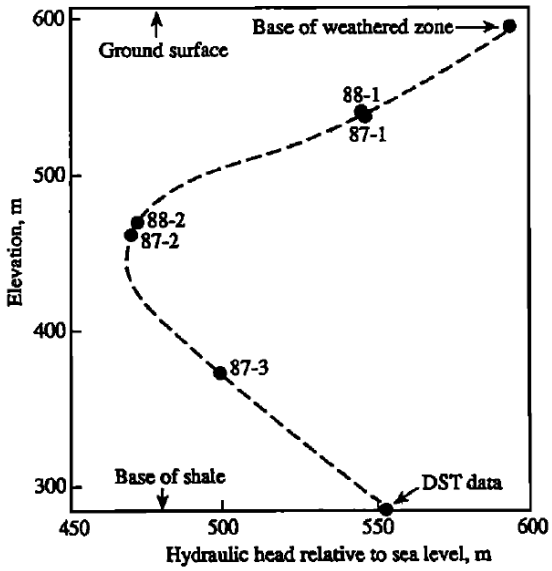

Figure 9. Hydraulic head profile in the Pierre Shale in North Dakota showing underpressurized conditions (from Neuzil 1993)

Table 12. Properties and distribution of the clay-rich formations in the USA (adapted from Gonzales and Johnson (1984) and other studies)

Property	Value	Formation	Location	Source
Total porosity (-)	0.05 to 0.18	Huron member Ohio Shale	Ohio-Kentucky	Soeder (1988)
	0.02 to 0.11	Ordovician	Ontario	Sykes et al. (2008)
	0.134	Pierre Shale	South Dakota	Olgaard et al. (1995)
	0.35 to 0.45	Pierre Shale	Saskatchewan	Smith et al. (2013)
	0.02 to 0.01	Trenton Group	Ontario	Gartner Lee Limited (2008)
Accessible porosity (-)	0.07 to 0.08	Wilcox	Louisiana	Kwon et al. (2004)
	0.04 to 0.1	Pierre Shale	South Dakota	Bredehoeft et al. (1983)
Hydraulic conductivity (m s^{-1})	8e-12 to 5.2e-11	Ordovician	Ontario	Sykes et al. (2008)
	4e-12 to 1e-11	Pierre Shale	South Dakota	Bredehoeft et al. (1983)
	1e-14 to 1e-13	Pierre Shale	South Dakota	Neuzil (1993)
	2E-12	Pierre Shale	South Dakota	Neuzil (1986)
	2e-16 to 2e-10	Trenton Group	Ontario	Beauheim et al. (2014), Clark et al. (2013)
	8e-13 to 2e-12	Trenton Group	Ontario	Gartner Lee Limited (2008)
	7.9e-14 to 8.2e-11	Huron member Ohio Shale	Ohio-Kentucky	Soeder (1988)
	5.8e-11 to 1.9e-10	Marcellus	West Virginia	Soeder (1988)
	3e-15 to 3e-12	Wilcox	Louisiana	Kwon et al. (2004)
Specific storativity (m^{-1})	1.3e-6 to 1.2e-4	Ordovician	Ontario	Sykes et al. (2008)
	8.0e-7	Pierre Shale	South Dakota	Neuzil (1986)
	2.69e-5 to 3.60e-5	Pierre Shale	South Dakota	Bredehoeft et al. (1983)
	1.1e-5 to 2.4 e-5	Pierre Shale	Saskatchewan	Smith et al. (2013)
	1.2e-6 to 1.3e-6	Trenton Group	Ontario	Gartner Lee Limited (2008)

3.4.4 Excavated Disturbed Zone (EDZ)

A major concern in post-closure safety evaluations of the repository system is the potential for hydromechanical perturbations caused by excavation. These perturbations are found within the excavation damaged zone (EDZ) around the repository tunnels and access shaft. The EDZ is primarily caused by redistribution of *in situ* stresses and rearrangement of rock structures (Tsang et al. 2012). Field investigations conducted at underground laboratories such as at Mont Terri (Switzerland) and Bure (France) have shown that the permeability of the EDZ can be one or more orders of magnitude higher than the unaltered argillaceous rock. This is primarily caused by the higher concentration of macro- and microfractures. For these conditions, the EDZ could then act as a preferential flow path for advective transport and thereby speed up radionuclide migration toward the biosphere. The EZD properties and their evolution over time have been analyzed in laboratory and field studies (Bossart et al. 2004; Baechler et al. 2011; Armand et al. 2013). These investigations suggest that a partial or complete self-sealing of fractures due to clay swelling and creep within the EDZ is possible after a certain amount of time. The self-sealing process can potentially decrease the EDZ permeability over time, which may eventually return to the values of the unaltered rock. However, the mechanisms and the time evolution of self-healing is still a matter of research, and at this point models simply assign constant permeability values for base-case scenarios. For the reference case described in this report, we followed the same simplified approach: the permeability in the EDZ is assumed constant in time with a value equal to 1×10^{-18} m^2. This value, which is 20 times higher than the unaltered argillaceous rock permeability, was used in previous performance assessment studies (ANDRA 2005; Genty et al. 2011), and more recently by Bianchi et al. (2013; 2014) The thicknesses of the EDZ around horizontal tunnels and the shaft in the reference case is assumed equal to 1.2 times the radius of the corresponding excavation (with a range of 0.8 to 1.6). This value is comparable to observations conducted at the Mont Terri in the Opalinus Clay (Bossart et al. 2004). The same thickness was also used in the simulations presented in Bianchi et al. (2013; 2014).

3.4.5 Radionuclide Transport Mechanisms in the Host Formation and EDZ

Bianchi et al. (2013; 2014) conducted numerical simulations of groundwater flow and radionuclide transport to understand factors controlling transport behavior within a generic HLW repository in an argillaceous formation. These simulations are based on simplified 2-D representation of the repository, including one horizontal emplacement tunnel, a vertical shaft, and cross section of the argillaceous host formation. Several scenarios were simulated to study the influence of several factors on transport behavior, including the hydraulic gradient in the host rock, the presence of pressure anomalies, the thickness of the EDZ, and its hydraulic properties. In their base case, these authors considered a vertical upward hydraulic gradient (1 m/m) resulting from imposing specified heads as boundary conditions at the top and bottom of the argillaceous formation, as well as hydrogeological parameters with values analogous to those presented for this reference case. The simulated flow field and the spatial distribution of the Peclet number (*Pe*) for the base-case scenario is considered in Bianchi et al. (2013; 2014), as shown in Figure 10.

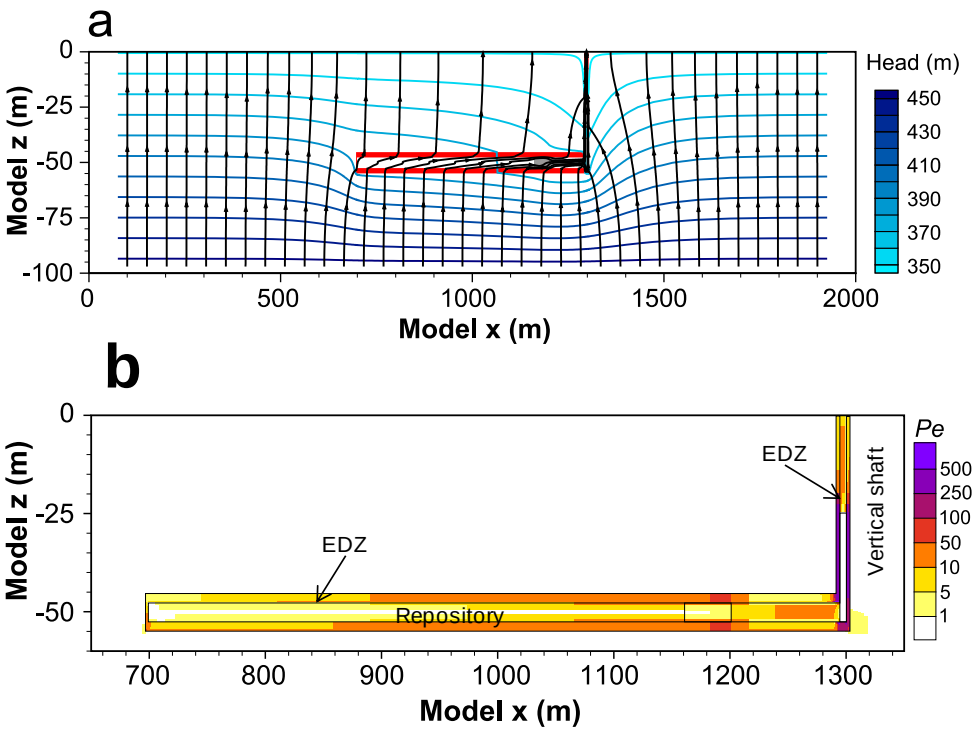

Figure 10. Simulated steady-state flow field (a) and Pe spatial distribution (b) in the base case scenario considered in Bianchi et al. (2013, 2014). The EZD is shown in red (a). (Modified from Bianchi et al. 2014).

The Peclet number was used to investigate whether and where transport in the simulated flow fields is driven by advection ($Pe > 10$) or molecular diffusion ($Pe < 1$). Results show (Figure 10) that radionuclide transport is driven by molecular diffusion in the argillaceous formation and (mostly) by advection in the EDZ. Diffusion is predominant in the emplacement tunnel and in the bentonite seals, while advective transport is prevalent in the more permeable tunnels backfill. In most of the simulated scenarios, the EDZ plays a major role as a preferential flow path for radionuclide transport. When the EDZ is not taken into account, transport is dominated by molecular diffusion in almost all the components of the simulated domain. On the other hand, in these simulations, the host rock, EDZ, and EBS are assumed fully saturated, and therefore these results have to be considered conservative with respect to the safety performance of the repository system. In particular, processes such as the self-sealing of the EDZ and consolidation of clay components in the EBS, may prevent preferential flow along the EDZ (Hansen et al. 2010). Moreover, advective transport along the EDZ and the access shaft may be insignificant due to a limited amount of water inflow from the argillite formation (Blümling et al., 2007; Hansen et al. 2010). All these aspects need to be further investigated after a site is identified. At this stage, the presented reference case considers diffusive transport in the argillaceous formation. This scenario corresponds to the "Nominal Scenario, Pathway 2" proposed by Hansen et al. (2010), in which diffusion is the prevalent mechanism moving radionuclides upward from the repository, through the NBS, to a shallow aquifer from which they are pumped to the biosphere. In this scenario, radionuclide transport is expected to be delayed by the reducing environment in the host rock and by sorption. Radioactive decay is also taken into account.

3.4.6 Chemical Properties

Chemical properties including mineralogical composition, water chemistry, diffusion and sorption coefficients are critical for evaluating the migration of radionuclides in host rocks. Some reference values of these properties are given below.

3.4.6.1 Mineralogical Composition

Some shales and argillites that are candidate host rocks for HLW disposal have been studied extensively, such as the Opalinus Clay at Mont Terri (Switzerland) (Thury 2002). Table 13 lists the mineralogical composition of Opalinus Clay. The measured mineralogical composition of Opalinus Clay varies remarkably, probably because of the spatial heterogeneity in mineralogical composition and the analytical method used. For example, Bossart (2011) summarized measured mineralogical composition from Waber et al. (1998), De Canniere (1997), Thury and Bossart (1999), and NAGRA (2003), and reported the mixed layer illite/smectite ranging from 5% to 11%. However, Lauber et al. (2000) reported the illite/smectite mixed layer ranging from 14% to 22%. The mineralogical compositions listed in Table 13 are the average of the Bossart (2011) and Lauber et al. (2000).

Table 13. Mineral volume fraction (dimensionless, ratio of the volume for a mineral to the total volume of medium) of Opalinus Clay (Bossart 2011; Lauber et al. 2000).

Mineral	Opalinus Clay
Calcite	0.093
Dolomite	0.050
Illite	0.273
Kaolinite	0.186
Smectite	0.035
Chlorite	0.076
Quartz	0.111
K-Feldspar	0.015
Siderite	0.020
Ankerite	0.045

3.4.6.2 Pore-water Chemistry

Pore-water chemistry in shale formations can be variable and hard to obtain, due to their low volumes and difficulties in extraction. Studies by Fernández et al. (2007) and Turrero et al. (2006) provide fairly comprehensive chemical characterizations of pore-waters for the Opalinus Clay (Switzerland) and an Oligocene-Miocene Clay from Spain. Very few sources relevant to clay formations in the USA can be found. Perry (2014) reported Cl concentration increase with depth, which is useful for delineating the evaporation trend, although he did not report a complete pore-water composition. The information in Perry (2014) is mostly limited to waters extracted from shale samples in deep weathered zones (e.g., Cody shale), groundwater from seeps and springs (e.g., Mancos shale), and production waters from oil field wells (e.g., Pierre shale). Water chemistries should preferably be constrained to extractions from rock samples relevant to repository depths. Moreover, samples should be well characterized and obtained at various formations depths to resolve chemical variability (both major elements and isotopes) and the extent of or lack of mixing with shallower groundwaters. The composition of pore-waters from Turrero et al. (2006) is shown in Figure 11. Perry (2014b) compiled chloride chemistry of various pore-waters collected from shale formations.

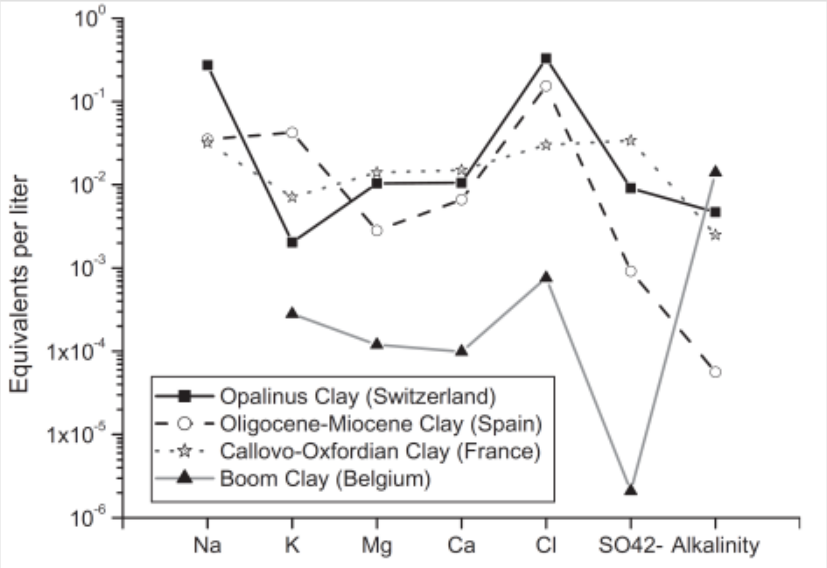

Figure 11. Composition of pore-waters in different argillaceous formations (from Turrero et al. 2006)

Fernandez et al. (2007) presented another study that provides data on the pore-water composition of the Opalinus Clay. They conducted five onsite water sampling campaigns from borehole BDI-B1. The average concentrations of these five campaigns are shown in Table 14.

Table 14. Pore-water composition of the Opalinus Clay.

	Opalinus Clay (Fernandez et al., 2007)
pH	7.40
Eh	0.268
Cl	3.32E-01
SO_4^{-2}	1.86E-02
HCO_3^-	5.18E-03
Ca^{+2}	2.26E-02
Mg^{+2}	2.09E-02
Na^+	2.76E-01
K^+	2.16E-03
Fe^{+2}	3.46E-06
$SiO_2(aq)$	1.10E-04
AlO_2^-	3.89E-08
F-	1.68E-05
Br-	3.2E-04
$O_2(aq)$	1.07E-41
UO_2^{+2}	1E-10

3.4.7 Diffusion Coefficients in the Argillaceous Host Rock

Diffusive transport of sorbing radionuclides in the reference argillaceous formation is defined by Fick's second law:

$$\varepsilon R \frac{\partial C}{\partial t} = \nabla \cdot (D_e \nabla C) \quad (7)$$

where C is concentration, t is the time, ε is the effective porosity, D_e is effective diffusion coefficient and R is retardation factor.

The effective diffusion coefficient takes into account the fact that in porous media the diffusion process is slower than in free water due to longer diffusive paths. D_e can then be described by the following equation:

$$D_e = \varepsilon D_p = \varepsilon \tau D_w \quad (8)$$

where D_p is the pore-water diffusion coefficient, τ is a geometrical factor representing the tortuosity of the diffusive paths in the porous medium, and D_w is the molecular diffusion coefficient in water. A uniform value equal to 0.1 is specified for tortuosity in the reference case.

Previous studies collected and reported datasets of diffusive parameters from argillaceous formations (e.g., Aertsens et al. 2004; van Loon et al. 2004a and 2004b; Descostes et al. 2008; Appelo et al. 2007). A summary of the diffusion parameters collected in clay-rock formations available in the literature was presented by Zheng et al. (2011b). For example, the D_e of ^{22}Na and ^{85}Sr in the Opalinus Clay range from 1.20×10^{-11} m^2/s to 6.0×10^{-11} m^2/s for ^{22}Na and from 1.4×10^{-11} m^2/s to 2.4×10^{-11} m^2/s for ^{85}Sr. Measurements of D_e of iodide in the Boom Clay along a depth interval of about 100 m range between 9.1×10^{-11} m^2/s and 5.2×10^{-10} m^2/s, with an average value of 1.6×10^{-10} m^2/s and a standard deviation of 9.0×10^{-11} m^2/s (Huysmans and Dassargues 2006). Laboratory scale experiments also showed that D_e is anisotropic; Samper et al. (2008), for instance, found that the anisotropy ratio e of D_e for HTO in a cylindrical rock sample of Callovo-Oxfordian argillite is between 0.26 and 0.56.

For the reference case described in this report, the water diffusion coefficient of generic radionuclide is assumed to be equal to 1.08×10^{-9} m^2/s (Bianchi et al. 2013; 2014), and with radionuclide-specific effects (e.g., due to size and charge) not considered at this stage. This value is similar to the diffusion coefficient of iodine, which is abundant in radioactive waste. Since iodine is also highly mobile in the solute phase, the assumed value is a conservative choice with respect to the safety performance of the repository system. Compound-specific diffusion coefficients will be considered in future stages of the repository performance assessment.

3.4.7.1 Sorption Data

Modeling sorption via linear sorption isotherm, i.e. distribution coefficient (K_d) is widely used in performance-assessment-level model. Because K_d depends not only on the properties of the adsorbate (i.e. radionuclides) but also adsorbents (i.e. host rock), it varies a great deal and is affected by many factors. For example, the plutonium K_d value was correlated to parameters specifying the aqueous chemical conditions and solid characteristics, using the data from Glover et al. (1976). This data set provides sorption data and a quantitative specification of the mineral phase and solution chemistry associated with each sorption experiment. The correlation indicates that the main controls on sorption are the soluble (or dissolved) carbon content (DC), the clay content (CC), the inorganic carbonate content (i.e., the $CaCO_3$ content) (IC), the pH, and the solution electrical conductivity (EC). These variables are correlated with the plutonium sorption K_d value based on

$$K_d = A_0 + A_1 CC^2 + A_2 CC^2 DC^2 + A_3 IC^2 + A_4 IC^2 (7 - pH)^2 + EC^2 \quad (9)$$

where K_d is in mL/g; DC is in meq/L; CC is in percent; IC is in percent; pH is dimensionless; and EC is in mmoh/cm.

McKinley and Scholits (1993) compiled and compared different sorption databases for argillites. A subset of their compilation is given in Table 15. Miller and Wang (2012) also reviewed sorption coefficients for some argillites.

Table 15. Distribution coefficient (K_d) for argillite from different database complied from different sources (McKinley and Scholits,1993).

Database: Sorbing material:	KBS-3 Bento-nite	NAGRA Bento-nite	AECL Bento-nite/sand	PAGIS Bento-nite	SKI Bento-nite	TVO Bento-nite	NRPB Clay	NRC Clay, soil shale	NAGRA Clay	PSE Sedi-ment	DOE, U.K. Clay
Cs	0.12	0.2	0.35	0.15	0.02	1	0.3	0.100	5	0.02	1
Sr	0.06	0.2	0.05		0.005	3	0.03	0.020			0.05
C_i		0.005							0.05	0	0.002
I	0.013	0.005	$8.5 \cdot 10^{-6}$		0.001		0	0	0.005	0	0.01
Se		0.005	0.004	0.02			0.03	0.005	0.005	0.0001	
Ni		1	0.012		0.1				0.5	0.01	0.05
Pd		0.005	0.012				0.3		0.5	0.1	
Sn		0.05	0.017				0.3	0.100	0.5	0.13	0.1
Zr		5	0.2	0.2	0.1		0.2	0.500	5	0.05	0.1
Tc	0.002	0.25	$9 \cdot 10^{-5}$	0.02	0.05		0	0.0004	0.25	0.001	0.04
Am	29.4	5	0.3	2	7	2.9	0.080	10	0.07	10	
Np	0.6	1	0.03	0.15	1	1	0.03	0.010	5	0.005	0.05
Pu	16.8	5	0.15	1.5	4	1	0.100	5	0.07	1	
Th	23.5	1	0.065	0.2	1	6	14.3	0.500	10	1	50
U	0.12	1	0.1	0.09	0.2	0.09	0.3	0.020	5	0.00002	0.2

4. Biosphere

The biosphere representation is usually dependent on regulatory guidance and specific scenarios for potential pathways towards near-surface receptors of contaminants (e.g., shallow aquifers, well water). The conceptualization of the biosphere is typically specified by regulation and can vary between different national radioactive waste disposal programs. For the reference case, the biosphere conceptualization is based on the International Atomic Energy Agency (IAEA) BIOMASS Example Reference Biosphere 1B (ERB 1B) dose model (IAEA 2003, Sections A.3.2 and C.2.6.1). The ERB 1B dose model assumes that the receptor is an individual adult who obtains drinking water from a pumping well drilled into the aquifer above the argillaceous host rock. Dissolved radionuclide concentrations in the aquifer are converted to estimates of annual dose to the receptor (dose from each radionuclide and total dose) using ERB 1B dose model parameters, which include the well pumping rate, the water consumption rate of the receptor, and radionuclide-specific dose conversion factors. Determination of dose model parameter values depends on the characteristics of the biosphere (e.g., climate) and the habits of the population (receptor) in that biosphere. Dose model parameters are not currently specified, but will be determined as the PA model matures.

5. Concluding Remark

In the past several years, under the UFDC, various kinds of models have been developed for repositories in argillaceous rock to demonstrate the modeling capability, understand the spatial and temporal alteration in the EBS bentonite and host rock, and evaluate different scenarios. However, the assumptions and the properties used in these models are not necessarily consistent, which not only make it difficult for inter-model comparison, but also compromises the applicability of the lessons learned in one model to another model. The establishment of a reference case would therefore be helpful to set up a baseline for model

development. A generic salt repository reference case was developed in Freeze et al. (2013) and a generic argillite repository reference case is presented in this report. The establishment of a reference case requires the description of waste inventory, waste form, waste package, repository layout, and the properties of EBS backfill and host rock, and biosphere. This report focuses on documenting the relevant processes and properties of EBS bentonite and host rock, with a brief description other components such as waste inventory, waste form, waste package, repository layout, and biosphere. A thorough description of the generic argillite repository reference case will be given in Jové Colón et al. (2014).

Some processes, including heat transport by advection and conduction, water flow by advection, vapor flow by diffusion, mechanical changes, and chemical reactions are known to be important for the EBS and host rock. Recent coupled THM and THMC simulations of these subsystems (Rutqvist et al. 2014a, 2014b; Zheng et al. 2014a, 2014b, 2014c) were very helpful in evaluating the importance of HM and MC coupling. HM coupling could be important because of its relevance to the time needed to fully saturate the EBS bentonite. The tentative conclusion from current THMC models is that MC coupling need not necessarily be directly included in the performance assessment model, but the variation in swelling capacity resulting from THMC models should be included in the performance assessment model for uncertainty analysis. Moreover, when site-specific data are available, coupled THMC models are warranted before determining whether to neglect MC coupling.

Parameters needed to describe the relevant processes are presented in the report. Most parameters for EBS bentonite are taken from FEBEX bentonite (ENRESA 2000) and MX-80 bentonite (SKB 2006). Regarding the parameters for argillite and shale, we have obtained data from shales in the US for some hydrological parameters, but also used data from European argillites and shales, such as the Opalinus Clay, for chemical parameters.

Acknowledgments

Funding for this work was provided by the Used Fuel Disposition Campaign, Office of Nuclear Energy, of the U.S. Department of Energy under Contract Number DE-AC02-05CH11231 with Lawrence Berkeley National Laboratory.

Helpful discussion with Geoff Freeze, David Sevougian, and Yifeng Wang from Sandia National Laboratories (SNL) are greatly appreciated.

References

Aertsens, M., I. Wemaere and L. Wouters (2004). Spatial variability of transport parameters in the Boom Clay. Applied Clay Science 26: 37–45.

Allard, B. (1985). Radionuclide sorption on concrete. NAGRA (Natl. Coop. Disposal Radioactive Waste), Baden. Nagra NTB 85-21. 13 pp.

ANDRA (2005). "Dossier 2005 Argile", Tome: Evaluation of the feasibility of a geological repository in an argillaceous formation. Andra Report Series.

Appelo, C. A. J. and P. Wersin (2007). Multicomponent diffusion modeling in clay systems with application to the diffusion of tritium, iodide, and sodium in opalinus clay. Environmental Science & Technology 41: 5002–5007.

Armand, G., A. Noiret, J. Zghondi, and D.M. Seyedi. (2013). Short- and long-term behaviors of drifts in the Callovo-Oxfordian claystone at the Meuse/Haute-Marne Underground Research Laboratory. Journal of Rock Mechanics and Geotechnical Engineering 5, no. 3: 221-230.

Baechler, S., J.M. Lavanchy, G. Armand, M. Cruchaudet. (2011). Characterisation of the hydraulic properties within the EDZ around drifts at level -490 m of the Meuse/Haute-Marne URL: a methodology for consistent interpretation of hydraulic tests. Physics and Chemistry of the Earth, no. 17: 1922-1931.

Beauheim R. L., R.M. Roberts, J.D. Avis (2014). Hydraulic testing of low-permeability Silurian and Ordovician strata, Michigan Basin, southwestern Ontario, Journal of Hydrology, Volume 509, 13 Pages 163-178.

Bernot P. (2005). Dissolved concentration limits for radioactive elements. ANL-WIS-MD-000010. July 2005.

Bianchi, M., H.-H., Liu, and J. T. Birkholzer. (2013). Diffusion Modeling in a Clay Repository: FY13 Report. . FCRD-UFD-2013-000228 Report, Lawrence Berkeley National Laboratory, Berkeley, USA.

Bianchi, M., H.-H., Liu, and J. T. Birkholzer. (2014). Radionuclide Transport Behavior in a Generic Geological Radioactive Waste Repository. Groundwater. doi: 10.1111/gwat.12171.

Blümling, P., F. Bernier, P. Lebon, and C.D. Martin. (2007). The excavation damaged zone in clay formations: Time-dependent behaviour and influence on performance assessment. Physics and Chemistry of the Earth 32: 588–599.

Börgesson, L. and J. Hernelind. (2005). Hydraulic bentonite/rock interactions in FEBEX experiment. In: Advances in Understanding Engineered Clay Barriers (E.E. Alonso and A. Ledesma, eds), pp. 391-412. Taylor & Francis Group, London, ISBN 04 1536 544 9.

Börgesson, L., O. Karnland, L. E. Johannesson and D. Gunnarsson. (2006). Current Status of SKB's Research, Development and Demonstration Programme on Buffer, Backfill and Seals. A report prepared by SKB for United Kingdom Nirex Ltd., SKB IC-122.

Bossart P. (2011) Characteristics of the Opalinus Clay at Mont Terri, http://www.mont-terri.ch/internet/mont-terri/en/home/geology/key_characteristics.html

Bossart, P., T. Trick, P.M. Meierand, and J.-C. Mayor. (2004). Structural and hydrogeological Characterization of the excavation-disturbed zone in the Opalinus Clay, Mont Terri Project, Switzerland. Applied Clay Science 26, no. 1-4: 429– 448.

Brandberg, F. and K. Skagius. (1991). Porosity, sorption and diffusivity data complied for the SKB 91 study. SKB technical report 91-16.

Bradbury, M.H. and B. Baeyens. (2002). Porewater chemistry in compacted re-saturated MX-80 bentonite: physico-chemical characterisation and geochemical modelling. PSI Bericht 02–10, Villigen PSI and NTB 01–08, Nagra, Wettingen, Switzerland.

Bradbury, M. H. and B. Baeyens. (2003a). Porewater chemistry in compacted re-saturated MX-80 bentonite. Journal of Contaminant Hydrology 61(1–4): 329-338.

Bradbury M. and B. Baeyens. (2003b). Near Field Sorption Data Bases for Compacted MX-80 Bentonite for Performance Assessment of a High- Level Radioactive Waste Repository in Opalinus Clay Host Rock. PSI Bericht Nr. 03-07 August 2003 ISSIN 1019-0643.

Bredehoeft, J. D., C. E. Neuzil, and P. C. D. Milly. (1983). Regional flow in the Dakota Aquifer: A study of the role of confining layers, U.S. Geol. Surv. Water Supply Pap., 2237, 1-45.

Buhmann. D., A. Nies and R. Storck. (1991). Systemanalyse Mischkonzept, Technischer Anhang 7. GSF (Ges. Strahlen-/Unweltforsch.), Braunschweig, KWA No. 5702A, 200 pp.

Buck, E. C., J. L. Jerden and R. S. Wittman. (2013). Coupling the Mixed Potential and Radiolysis Models for Used Fuel Degradation, FCRD-UFD-2013-000290, PNNL Report PNNL-22701, 30 pp.

Caporuscio F.A., Cheshire, M. C., McCarney, M. (2012) Bentonite Clay Evolution at Elevated Pressures and Temperatures: An experimental study for generic nuclear repositories, 2012 AGU fall meeting.

Cheshire, M. C., Caporuscio, F. A., Jové-Colon, C. and McCarney, M. K. (2013) Alteration of clinoptilolite into high-silica analcime within a bentonite barrier system under used nuclear fuel repository conditions. International High-Level Radioactive Waste Management (2013 IHLRWM). Albuquerque, NM.

Cheshire, M., F. Caporuscio, M. Rearick, C. Jové Colón and M. K. McCarney (2014). Bentonite evolution at elevated pressures and temperatures: an experimental study for generic nuclear repository designs. American Mineralogist: in press.

Carter, J. T., A. J. Luptak, J. Gastelum, C. Stockman, and A. Miller (2012). *Fuel Cycle Potential Waste Inventory for Disposition*. FCRD-USED-2010-000031, Rev. 5. U.S. Department of Energy, Office of Used Nuclear Fuel Disposition, Washington, DC.

Clayton, D., G. Freeze, T. Hadgu, E. Hardin, J. Lee, J. Prouty, R. Rogers, W.M. Nutt, J. Birkholzer, H.H. Liu, L. Zheng, and S. Chu (2011). *Generic Disposal System Modeling – Fiscal Year 2011 Progress Report.* FCRD-USED-2011-000184, SAND2011-5828P. U.S. Department of Energy, Office of Nuclear Energy, Used Fuel Disposition Campaign, Washington, DC.

Croisé, J., L. Schlickenrieder, P. Marschall, J.Y. Boisson, P. Vogel, and S. Yamamoto. (2004). Hydrogeological investigations in a low permeability claystone formation: the Mont Terri Rock Laboratory. Physics and Chemistry of the Earth Parts A/B/C 29, no. 1:3-15.

Clark I.D., T. Al, M. Jensen, L. Kennell, M. Mazurek, R. Mohapatra, K.G. Ravent (2013). Paleozoic-age brine and authigenic helium preserved in an Ordovician shale aquiclude. Geology, 41, pp. 951–954.

Curtis, E. and Wersin, P. (2002). Assessment of porewater chemistry in the bentonite buffer for the Swiss SF/HLW repository. PSI Bericht, Paul Scherrer Institut, Villigen, Nagra Technical Report NTB 02-09, Nagra, Wettingen, Switzerland.

Descostes, M., V. Blin, F. Bazer-Bachi, P. Meier, B. Grenut, J. Radwan, M.L. Schlegel, S. Buschaert, D. Coelho E. and Tevissen (2008). Diffusion of anionic species in Callovo-Oxfordian argillites and Oxfordian limestones (Meuse/Haute–Marne, France). Applied Geochemistry 23: 655–677.

De Canniere, P. (1997). Measurements of Eh on slurries of Opalinus Clay, Mont Terri. SCK•CEN. Mont Terri Project, Technical Note TN 96-32 (internal unpublished report).

De Windt, L., F. Marsal, E. Tinseau and D. Pellegrini (2008). Reactive transport modeling of geochemical interactions at a concrete/argillite interface, Tournemire site (France). Physics and Chemistry of the Earth, Parts A/B/C 33, Supplement 1(0): S295-S305.

Einstein, H., (2000). Tunnels in Opalinus Clayshale—a review of case histories and new developments. Tunnelling and Underground Space Technology, 15(1): p. 13-29.

ENRESA (2000). Full-scale engineered barriers experiment for a deep geological repository in crystalline host rock FEBEX Project, European Commission**:** 403.

Ewart. F.T.. Pugh, S.Y.R., Wisbey. S.J. and Woodwark. D.R.. (1988). Chemical and microbiological effects in the near field - Current status. Nirex Ltd., Harwell, NSS/G103. 32 pp.

Fernández, A., Cuevas, J., Rivas, P., (2001). Pore-water chemistry of the FEBEX bentonite. Mat. Res. Soc. Symp. Proc. 663, 573–588.

Fernández, A. M., B. Baeyens, M. Bradbury and P. Rivas (2004). Analysis of the porewater chemical composition of a Spanish compacted bentonite used in an engineered barrier. Physics and Chemistry of the Earth, Parts A/B/C 29(1): 105-118.

Fernández, A. M., M. Turrero, D. Sánchez, A. Yllera, A. Melón, M. Sánchez, J. Peña, A. Garralón, P. Rivas and P. Bossart (2007). On site measurements of the redox and carbonate system parameters in the low-permeability Opalinus Clay formation at the Mont Terri Rock Laboratory. Physics and Chemistry of the Earth, Parts A/B/C 32(1): 181-195.

Freeze, G., M. Voegele, P. Vaughn, J. Prouty, W.M. Nutt, E. Hardin, and S.D. Sevougian (2013). *Generic Deep Geologic Disposal Safety Case.* FCRD-UFD-2012-000146 Rev. 1, SAND2013-0974P. Sandia National Laboratories, Albuquerque, NM.

Gaboreau, S., C. Lerouge, S. Dewonck, Y. Linard, X. Bourbon, C. Fialips, A. Mazurier, D. Prêt, D. Borschneck and V. Montouillout (2012). In-situ interaction of cement paste and shotcrete with claystones in a deep disposal context. American Journal of Science 312(3): 314-356.

García-Gutiérrez, M., T. Missana, M. Mingarro, J. Samper, Z. Dai and J. Molinero (2001). Solute transport properties of compacted Ca-bentonite used in FEBEX project. Journal of Contaminant Hydrology 47(2–4): 127-137.

Gartner Lee Limited (2008). Phase I Regional Geology, Southern Ontario. OPG's Deep Geologic Repository for Low & Intermediate Level Waste, Supporting Techinical Report. GLL 61-123; OPG 00216-REP-01300-00007-R00.

Gaucher, E. C. and P. Blanc 2006. Cement/clay interactions – A review: Experiments, natural analogues, and modeling. Waste Management 26(7): 776-788.

Genty, A., C. Le Potier, and S. Gounand. (2011). Analysis of the Excavation Deviations Impact on Geological Radioactive Waste Repository Performance. Geotechnical and Geological Engineering 29, no. 4: 537-554.

Glover P. A., Miner F. J. and Polzer W. O. (1976). Plutonium and Americium behavior in the soil/water environment. I. sorption of Plutonium and Americium by soils. In Proceedings of Actinide-Sediment Reactions Working Meeting, Seattle, Washington. pp. 225-254, BNWL-2117, Battelle Pacific Northwest Laboratories, Richland, Washington.

Greenberg, H. R. J. Wen, T. A. Buscheck, (2013). Scoping Thermal Analysis of Alternative Dual-Purpose Canister Disposal Concepts. LLNL-TR-639869.

Greene, S.R., J.S. Medford, and S.A. Macy, (2013). Storage and Transport Cask Data For Used Commercial Nuclear Fuel (2013 U.S. Edition), Report ATI-TR-130472013, EnergX, LLC: Oak Ridge, TN. 314 pp.

Gonzales, S. and K.S. Johnson, (1984). Shale and other argillaceous strata in the United States. Oak Ridge National Laboratory. ORNL/Sub/84-64794/1.

Hansen, F.D., E.L. Hardin, R. P. Rechard, G. A. Freeze, D.C. Sassani, P.V. Brady, C. M. Stone, M. J. Martinez, J. F. Holland, T. Dewers, K.N. Gaither, S. R. Sobolik, and R. T. Cygan, (2010). Shale Disposal of U.S. High-Level Radioactive Waste. SAND2010-2843. Albuquerque, NM: Sandia National Laboratories.

Hardin, E., J. Blink, H. Greenberg, M. Sutton, F. Massimiliano, J. Carter, M. Dupont, R. Howard, (2011). Generic Repository Design Concepts and Thermal Analysis (FY11). Sandia report SAND2011-6202.

Hardin, E., T. Hadgu, D. Clayton, R. Howard, H. Greenberg, J. Blink, M. Sharma, M. Sutton, J. Carter, M. Dupont, and P. Rodwell, (2012). *Repository Reference Disposal Concepts and Thermal Load Management Analysis.* FCRD-UFD-2012-000219 Rev. 2. U.S. Department of Energy, Office of Used Nuclear Fuel Disposition, Washington, DC.

Hardin, E., Clayton, D., Howard, R., Scaglione, J.M., Pierce, E., Banerjee, K., Voegele, M.D., Greenberg, H., Wen, J., Buscheck, T.A., Carter, J.T., Severynse, T., Nutt, W.M., (2013). Preliminary Report on Dual-Purpose Canister Disposal Alternatives (FY13), August, 2013, FCRD-UFD-2013-000171 Rev. 0.

Hardin, E., (2014). Review of Underground Construction Methods and Opening Stability for Repositories in Clay/Shale Media (FCRD-UFD-2014-000330), Sandia National Laboratories: Albuquerque, NM. 48 pp.

Hicks, T.W., White, M.J. and Hooker, P.J. (2009). Role of Bentonite in Determination of Thermal Limits on Geological Disposal Facility Design, Report 0883-1, Version 2, Falson Sciences Ltd., Rutland, UK, Sept. 2009.

Hökmark, H. (2004). Hydration of the bentonite buffer in a KBS-3 repository. Applied Clay Science 26(1–4): 219-233.

Houseworth J., Jonny Rutqvist, Daisuke Asahina, Fei Chen, Victor Vilarrasa, H.H Liu, Jens Birkholzer. (2013). International Collaborations on FE Heater and HG-A Tests. Lawrence Berkeley National Laboratory November, 2013. FCRD-UFD-2014-000002.

Huysmans, M. and A. Dessargues (2006). Stochastic analysis of the effect of spatial variability of diffusion parameters on radionuclide transport in a low permeability clay layer. Hydrogeology Journal 14: 1094–1106.

Jové Colón, C.F., F.A. Caporuscio, S.S. Levy, J.A. Blink, H.R. Greenberg, W.G. Halsey, M. Fratoni, M. Sutton, T.J. Wolery, J. Rutqvist, H.H. Liu, J. Birkholzer, C.I. Steefel, and J. Galindez, (2011). Disposal Systems Evaluations and Tool Development - Engineered Barrier System (EBS) Evaluation, p. 1-192.

Jové Colón, C.F., J.A. Greathouse, S. Teich-McGoldrick, R.T. Cygan, T. Hadgu, J.E. Bean, M.J. Martinez, P.L. Hopkins, J.G. Argüello, F.D. Hansen, F.A. Caporuscio, and M. Cheshire, et al., (2012). Evaluation of Generic EBS Design Concepts and Process Models: Implications to EBS Design Optimization (FCRD-USED-2012-000140), 2012, U.S. Department of Energy. p. 250.

Jové Colón, C. J. A. Greathouse, S. Teich-McGoldrick, et al., (2013). EBS Model Development and Evaluation Report, FCRD-UFD-2013-000312.

Jové Colón, C., L. Zheng, J. Houseworth, et al. (2014). Evaluation of used fuel disposition in clay-bearing rock, FCRD-UFD-2014-000056.

JNC (2000). H12: Project to Establish the Scientific and Technical Basis for HLW Disposal in Japan. Second Progress Report on Research and Development for the Geological Disposal of HLW in Japan. Supporting Report 2: Repository Design and Engineering Technology. JNC TN1410 2000-003.

Kosakowski, G. and U. Berner (2013). The evolution of clay rock/cement interfaces in a cementitious repository for low- and intermediate level radioactive waste. Physics and Chemistry of the Earth, Parts A/B/C 64(0): 65-86.

Kwon, O., A. K. Kronenberg, A. F. Gangi, B. Johnson, and B. E. Herbert (2004). Permeability of illite-bearing shale: 1. Anisotropy and effects of clay content and loading, J. Geophys. Res., 109, B10205, doi:10.1029/2004JB003052.

Lauber, M., B. Baeyens and Bradbury, M. H. (2000). Physico-Chemical Characterisation and Sorption Measurements of Cs, Sr, Ni, Eu, Th, Sn and Se on Opalinus Clay from Mont Terri. PSI Bericht Nr. 00-10 December 2000 ISSN 1019-0643.

Lide, D.R., ed. (1999). CRC Handbook of Chemistry and Physics, CRC Press, Boca Raton, FL.

Liu, H.H., J. Houseworth, J. Rutqvist, L. Zheng, D.e Asahina, L. Li, V. Vilarrasa, F. Chen, S. Nakagawa, S. Finsterle, C. Doughty, T. Kneafsey and J. Birkholzer. (2013). Report on THMC modeling of the near field evolution of a generic clay repository: Model validation and demonstration, Lawrence Berkeley National Laboratory, August, 2013, FCRD-UFD-2013-0000244.

Man A. and Martino J.B. (2009). Thermal , hydraulic and mechanical properties of sealing materials. NWMO TR-2009-20. December 2009, Atomic Energy and Canada Limited.

Mazurek, M., F.J. Pearson, G. Volckaert, and H. Bock, Features, Events and Processes Evaluation Catalogue for Argillaceous Media, (2003). Organisation for Economic Co-operation and Development (OECD) - Nuclear Energy Agency (NEA): Paris, France. 379 pp.

McKinley, I. G. and A. Scholits (1993). A comparison of radionuclide sorption databases used in recent performance assessments. Journal of Contaminant Hydrology 13(1–4): 347-363.

Miller, A. W. and Y. Wang (2012). Radionuclide interaction with clays in dilute and heavily compacted systems: a critical review. Environmental Science & Technology 46(4): 1981-1994.

Nacarrow, D.J., Sumerling, T.J. and Ashton, J., (1988). Preliminary radiological assessments of low-level waste repositories. U.K. DOE (Dep. Environ.), London, Rep. DOE/RW/88.084,62 pp.

NAGRA (2002). Project Opalinus Clay: safety report. Demonstration of disposal feasibility for spent fuel, vitrified high-level waste and long-lived intermediate level waste (Entsorgungsnachweis). Nagra Technical Report NTB 02-05, Wettingen, Switzerland.

NAGRA (2003). Geosynthese. Nagra Technical Report NTB 02-03. Nagra, Wettingen, Switzerland.

Neuzil, C. E. (1986). Groundwater flow in low-permeability environments, Water Resour. Res., 22(8), 1163-1195.

Neuzil, C. E. (1993). Low fluid pressure within the Pierre Shale: A transient response to erosion, Water Resour. Res., 29(7), 2007–2020, doi:10.1029/ 93WR00406.

Neuzil, C. (2013). Can Shale Safely Host US Nuclear Waste? Eos, Transactions American Geophysical Union 94(30): 261-262.

Olgaard, D.L. Nueesch, R., Urai, J., (1995). Consolidation of water saturated shales at great depth under drained conditions. In: Fujii, T. (Ed.), Proceedings of the Congress of the International Society for Rock Mechanics, vol. 8, pp. 273– 277.

Ochs, M., B. Lothenbach, H. Wanner, H. Sato and M. Yui (2001). An integrated sorption–diffusion model for the calculation of consistent distribution and diffusion coefficients in compacted bentonite. Journal of Contaminant Hydrology 47(2–4): 283-296.

Perry, F.V., (2014a). Regional Geology: A GIS Database for Alternative Host Rocks and Potential Siting Guidelines (FCRD-UFD-2014-000068), LANL Unlimited Release Report LA-UR-14-203682014, Los Alamos National Laboratory: Los Alamos, NM.

Perry, F.V., (2014b). Survey of chloride concentrations in formation (pore) waters of crystalline rocks and shale, Fuel Cycle R&D, FCRD-UFD-2014-000514, Los Alamos Unlimited Release LA-UR-14-24761, 14 pp.

Pusch, R., Bluemling, P. and Johnson, L. (2003). Performance of strongly compressed MX-80 pellets under repository-like conditions, Applied Clay Science 23: 239– 244.

Pusch, R., Kasbohm, J. and Thao, H. T. M. (2010). Chemical stability of montmorillonite buffer clay under repository-like conditions—A synthesis of relevant experimental data. Applied Clay Science 47(1–2): 113-119.

Rutqvist, J., D. Barr, J. Birkholzer, K. Fujisaki, O. Kolditz, Q.-S. Liu, T. Fujita, W. Wang and C.-Y. Zhang (2009). A comparative simulation study of coupled THM processes and their effect on fractured rock permeability around nuclear waste repositories. Environmental Geology 57(6): 1347-1360.

Rutqvist, J., Y. Ijiri and H. Yamamoto (2011). Implementation of the Barcelona Basic Model into TOUGH–FLAC for simulations of the geomechanical behavior of unsaturated soils. Computers & Geosciences 37(6): 751-762.

Rutqvist, J., L. Zheng, F. Chen, H.-H. Liu and J. Birkholzer (2014a). Modeling of Coupled Thermo-Hydro-Mechanical Processes with Links to Geochemistry Associated with Bentonite-Backfilled Repository Tunnels in Clay Formations. Rock Mechanics and Rock Engineering 47(1): 167-186.

Rutqvist, J., L. Zheng, F. Chen, H.-H. Liu and J. Birkholzer (2014b). Investigation of coupled THMC process and reactive transport: FY14 progress. FCRD-UFD-2014-000497

Samper, J., Q. Yang, S. Yi, M. García-Gutiérrez, T. Missana, M. Mingarro, Ú. Alonso and J.L. Cormenzana (2008). Numerical modelling of large-scale solid-source diffusion experiment in Callovo-Oxfordian clay. Physics and Chemistry of the Earth 33 (Suppl. 1): S208–S215.

Sánchez, M., A. Gens and S. Olivella (2012). THM analysis of a large-scale heating test incorporating material fabric changes. International Journal for Numerical and Analytical Methods in Geomechanics 36(4): 391-421.

Schultz, L. G., (1965). Mineralogy and stratigraphy of the lower part of the Pierre Shale, South Dakota and Nebraska: U.S. Geol. Survey Prof. Paper 392-B, p. B1-B19.

Sevougian, S.D., G.A. Freeze, P. Vaughn, P. Mariner, and W.P. Gardner (2013). *Update to the Salt R&D Reference Case*. FCRD-UFD-2013-000368, SAND2013-8255P. Sandia National Laboratories, Albuquerque, NM.

Shurr, G.W. (1977). The Pierre Shale, Northern Great Plains; A Potential Isolation Medium for Radioactive Waste. United States Geological Survey Open File Report 77-776.

SKB (Svensk Kärnbränslehantering AB) (2006). Buffer and backfill process report for the safety assessment SR-Can, SKB Technical Report TR-06-18.

SKB (Svensk Kärnbränslehantering AB) (2010). *Data Report for the Safety Assessment SR-Site*. Technical Report TR-10-52. Swedish Nuclear Fuel and Waste Management Co., Stockholm, Sweden.

SNL (Sandia National Laboratories) 2007. *Radionuclide Screening*. ANL-WIS-MD-000006 REV 02, U.S. Department of Energy, Office of Civilian Radioactive Waste Management, Las Vegas, Nevada.

Smith, L. A., G. van der Kamp, M. J. Hendry (2013). A new technique for obtaining high-resolution pore pressure records in thick claystone aquitards and its use to determine in situ compressibility, Water Resour. Res., 49, 1–12, doi:10.1002/wrcr.20084.

Soeder, D.J., (1988). Porosity and permeability of eastern Devonian gas shale: Society of Petroleum Engineers Formation Evaluation, Society of Petroleum Engineers, v. 3, no. 2, p. 116–124, DOI 10.2118/15213–PA.

Sassani, D.C., C.F. Jové Colón, P. Weck, J.L. Jerden, K.E. Frey, T. Cruse, W.L. Ebert, E.C. Buck, R.S. Wittman, F.N. Skomurski, K.J. Cantrell, B.K. McNamara, and C.Z. Soderquist, Integration of EBS Models with Generic Disposal System Models (FCRD-UFD-2012-000277), 2012, Sandia National Laboratories: Albuquerque, NM., 145 pp.

Sykes E. A., J. F. Sykes, S. D. Normani, E. A. Sudicky and Y. J. Park. (2008). Phase I Hydrogeologic modelling. OPG's Deep Geologic Repository for Low & Intermediate Level Waste, Supporting Techinical Report. GLL 61-123; OPG 00216-REP-01300-00009-R00.

Thury, M. and Bossart, P. (1999): Results of the hydrogeological, geochemical and geotechnical experiments performed in the Opalinus Clay (1996-1997). Chapter 6.4 Organic Matter Characterisation of Rocks and Pore-waters. Geological report No. 23. Swiss Geological Survey.

Toutelot, H. A., (1962). Preliminary Investigation of the Geologic Setting and Chemical Composition of the Pierre Shale Great Plains Region, UNITED STATES GEOLOGICAL SURVEY PROFESSIONAL PAPER 390, 81 pp.

Tsang, C.-F., J.D. Barnichon, J.T. Birkholzer, , X.L. Li, H.H. Liu, X. Sillen, and T. Vietor. (2012). Coupled Thermo-Hydro-Mechanical Processes in the Near-Field of a High-Level Radioactive Waste Repository in Clay Formations. International Journal of Rock Mechanics and Mining Sciences 49: 31-44.

Turrero et al., (2006). M.J. Turrero, A.M. Fernández, J. Peña, M.D. Sánchez, P. Wersin, P. Bossart, M. Sánchez, A. Melón, A. Yllera, A. Garralón, P. Gómez, P. Hernán. Pore-water chemistry of a Paleogene continental mudrock in Spain and a Jurassic marine mudrock in Switzerland: sampling methods and geochemical interpretation. J. Iberian Geol., 32 (2006), pp. 233–258.

van Genuchten, M. T. (1980). A closed-form equation for predicting the hydraulic conductivity of unsaturated soils. Soil science society of America journal 44(5): 892-898.

van Loon, L.R., J.M. Soler, W. Muller and M.H. Bradbury (2004a). Anisotropic diffusion in layered argillaceous rocks: a case study with opalinus clay. Environmental Science & Technology 38: 5721–5728.

van Loon, L.R., P. Wersin, J.M. Soler, J. Eikenberg, T. Gimmi, P. Hernan, S. Dewonck and S. Savoye (2004b). In-situ diffusion of HTO, $^{22}Na^{+}$, Cs^{+} and I^{-} in Opalinus Clay at the Mont Terri underground rock laboratory. Radiochimica Acta 92: 757–763.

Vietor, T. (2012). Mont Terri Project - FE Experiment Modelling Kick-off Meeting. February 9, 2012, Mont Terri, Switzerland. NAGRA Technical Discussion TD-217.

Vieno, T. and Nordman, H., (1991). Safety analysis of the VLJ repository. Nuclear Waste Commission of Finnish Power Companies, Helsinki, Rep. YJT-91-12, 14 pp. (in Finnish).

Villar, M. V., M. Sánchez and A. Gens (2008). Behaviour of a bentonite barrier in the laboratory: Experimental results up to 80 years and numerical simulation. Physics and Chemistry of the Earth, Parts A/B/C 33, Supplement 1(0): S476-S485.

Waber, H.N., Mazurek, M. and Pearson, F.J. (1998). Opalinus Clay: reference porewater, mineralogy and porosity. NAGRA Internal Report.

Wersin P., Johnson, L.H. and McKinley, I.G. (2007). Performance of the bentonite barrier at temperature beyond 100°C: A critical review, Physics and Chemistry of the Earth 32: 780-788.

Wiborgh, M. and Lindgreen, M., (1987). SKA progress report. SKB (Swed. Nucl. Fuel & Waste Manage. Co.), Stockholm, SFR 87-09, 63 pp.

Zheng, L., J. Samper and L. Montenegro (2008). Inverse hydrochemical models of aqueous extracts tests. Physics and Chemistry of the Earth, Parts A/B/C 33(14–16): 1009-1018.

Zheng, L., J. Samper and L. Montenegro (2011a). A coupled THC model of the FEBEX in situ test with bentonite swelling and chemical and thermal osmosis. Journal of Contaminant Hydrology 126(1–2): 45-60.

Zheng, L., H.H. Liu, J. Birkoltzer and W.M. Nutt (2011b). Diffusion modeling in a generic clay repository. FCRD-LBNL-2011-SLM: 25

Zheng, L., James Houseworth, Carl Steefel, Jonny Rutqvist, Jens Birkholzer (2014a), Investigation of Coupled Processes and Impact of High Temperature Limits in Argillite Rock. FCRD-UFD-2014-000493

Zheng, L., J. Rutqvist, H.-H. Liu, J. T. Birkholzer and E. Sonnenthal (2014b). Model evaluation of geochemically induced swelling/shrinkage in argillaceous formations for nuclear waste disposal. Applied Clay Science 97–98(0): 24-32.

Zheng, L., Jonny Rutqvist, Harris Greenberg, Jens Birkholzer. (2014c). Model Evaluation of the Thermo-Hydrological-Mechanical Response in Argillaceous Sedimentary Rock Repository for Direct Disposal of Dual-Purpose Canisters. FCRD-UFDC-2014-000515.